Reactivity–Structure-Based Rate Estimation Rules for Alkyl Radical H Atom Shift and Alkenyl Radical Cycloaddition Reactions

ARTICLE *in* THE JOURNAL OF PHYSICAL CHEMISTRY A · JANUARY 2015

Impact Factor: 2.69 · DOI: 10.1021/jp511017z · Source: PubMed

3 AUTHORS:

Kun Wang
Stanford University
18 PUBLICATIONS **11** CITATIONS
SEE PROFILE

Stephanie M Villano
Colorado School of Mines
30 PUBLICATIONS **459** CITATIONS
SEE PROFILE

Anthony M Dean
Colorado School of Mines
158 PUBLICATIONS **3,933** CITATIONS
SEE PROFILE

THE JOURNAL OF PHYSICAL CHEMISTRY A

Article

pubs.acs.org/JPCA

Reactivity−Structure-Based Rate Estimation Rules for Alkyl Radical H Atom Shift and Alkenyl Radical Cycloaddition Reactions

Kun Wang, Stephanie M. Villano, and Anthony M. Dean*

Chemical and Biological Engineering Department, Colorado School of Mines, Olden, Colorado 80401, United States

Supporting Information

ABSTRACT: Intramolecular H atom shift reactions of alkyl radicals and cycloaddition reactions of alkenyl radicals are two important reaction classes in hydrocarbon combustion and pyrolysis. In this work, we derive high-pressure rate estimation rules that are based on the results of electronic structure calculations at the CBS-QB3 level of theory combined with transition state theory calculations. The rules for the H atom shift reactions of alkyl radicals cover the 1,2- up to the 1,7-H shifts. The rules for the cycloaddition reactions of alkenyl radicals are for both the endo- and exo-cycloaddition and include the formation of three- to seven-member ring products. The results are in good agreement with available experiment measurements and other theoretical studies. Both types of reactions proceed via cyclic transition state structures. The impact of ring size and substituent groups on pre-exponential factors and activation energies are discussed in the context of a Benson-type structure−reactivity relationship. Similar relationships between the pre-exponential factors and the number of internal rotors lost in formation of the transition state are derived for both H-shift and cycloaddition reactions. The activation energies are found to be more complicated. The ring strain contribution to the barrier is much lower for the exo-cycloaddition reactions than it is for the other two investigated reaction systems. The ring strains for the H-shift and endo-cycloaddition are similar to one another and are comparable to that of cycloalkanes for three- to six-member rings, but are significantly lower for the larger rings. The results suggest that the 1,6-H shift and 1,7-endo-cycloaddition reactions might be faster than previous estimates.

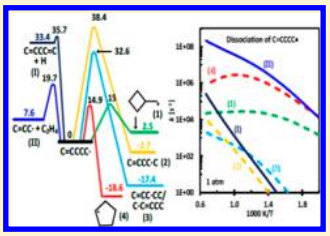

INTRODUCTION

Hydrocarbons, whether derived from petroleum or renewable sources, will be a primary fuel source for the foreseeable future. Because of this, there has been a long-standing interest in understanding their thermal decomposition. Detailed kinetic models that can accurately describe the oxidation and/or pyrolysis of hydrocarbons are a valuable tool that can be used to predict the performance of these fuels under varying conditions. Generally speaking, these mechanisms are very large, sometimes consisting of thousands of species and tens of thousands of reactions. To facilitate their development, the kinetic parameters for a given type of reaction are often assigned using rate estimation rules. In the past, many of these rules were assigned based on limited amounts of published data, either obtained by experiment or theoretical means. However, with the advent of more sophisticated computer hardware and more accurate electronic structure methods, it is now possible to use this approach to develop these rate constant rules by systematic calculations of a series of reactions for a given reaction class.

The purpose of this work is to derive rate estimation rules for the intramolecular H atom shift reactions of alkyl radicals and the cycloaddition reactions of alkenyl radicals. The commonality in these two reaction classes is that they both proceed through cyclic transition state structures. From the perspective of a Benson-type model,[1] these reactions may be considered to be intramolecular H-abstraction or addition reactions, respectively. Thus, their activation energies may be considered to consist of two parts: the activation energy of the corresponding bimolecular reaction plus the ring strain energy ($E_a = E_{bi} + E_{strain}$). Prior to any reliable experimental or theoretical studies, the ring strain energy was often assumed to be that of the corresponding cycloalkane.[1] However, recent work suggests that this analogy does not provide good estimates.[2−5] Pre-exponential factors were calculated from the entropy difference between the reactant and transition state. This difference should correlate with the loss of internal rotors in the cyclic transition state structure. While there have been several previous experimental and theoretical studies of both reaction classes, this work provides results for a large number of reactions using a consistent theoretical approach that permits development of a more complete structure−reactivity-based picture for these two reaction classes.

Intramolecular H atom shift reactions play an important role in hydrocarbon combustion and pyrolysis. These reactions compete with unimolecular β-scission as well as bimolecular reactions. They may modify the initial alkyl radical isomer population that is formed by H atom abstraction reactions from the parent hydrocarbon, thereby affecting both the rate and the

Special Issue: 100 Years of Combustion Kinetics at Argonne: A Festschrift for Lawrence B. Harding, Joe V. Michael, and Albert F. Wagner

Received: November 3, 2014
Revised: January 4, 2015

DOI: 10.1021/jp511017z
J. Phys. Chem. A XXXX, XXX, XXX−XXX

product distribution. There have been a number of prior experimental[6−15] and theoretical studies[16−22] on this reaction class. These data show that the 1,4- to 1,6-H atom shift reactions (that proceed via five- to seven-member ring transition states, respectively) are favored over the 1,2- and 1,3-shifts (via three- and four-member ring transition states). Several of these studies have provided rate estimation rules. Sirjean et al.[5] and Ratkiewicz et al.[23−25] developed rate rules for 1,4- to 1,6-H shift reactions. Matheu et al.[26] developed a set of rate rules for the 1,2- to 1,6-H shifts in alkyl radicals. In each of these cases, the rules were based on only a limited number of reactions, and no substituent effects were considered. Davis and Francisco[4,27] conducted thorough investigations on all possible H-shift reactions for linear and branched alkyl radicals using CBS-Q, G2, and G4 composite computational methods. The impact of abstraction site location, substituents, and transition-state configurations on the activation energy, pre-exponential factor, tunneling factor, and the overall rate coefficient was discussed. However, the authors did not generalize their results to provide the rate constant rules that are needed to generate self-consistent rate constants for inclusion in kinetic mechanisms.

Alkenyl radicals (where there is an alkyl radical site on an olefin) are formed by allylic radical addition to olefins or by H-abstraction from olefins. Once formed, they can isomerize via cycloaddition or H atom shift (preferably forming an allylic radical), β-scission, or undergo bimolecular reactions. The cycloaddition pathway is important because it may be an efficient route to form aromatics and ultimately to the formation of deposits or soot.[28] There are two possible addition sites (c.f., Scheme 1). Addition to the far vinylic carbon leads to a cycloalkyl radical; this is referred to as an endo-cycloaddition. Addition to the near vinylic carbon leads to a cycloalkyl-carbinyl radical; this is referred to as an exo-cycloaddition. Several prior studies have been conducted on these cycloaddition reactions or on the reverse ring opening reactions.[29−33] Baldwin[34] provided semiempirical rules to predict the relative ease of ring closure via the two pathways; the exo-cycloaddition reactions were found to be more favorable than the corresponding endo-addition. Matheu et al.[26] proposed high-pressure rate constants for the endo-cycloaddition to form five- and six-member ring radicals and for the exo-cycloaddition to form five-member ring radicals. The rate constant for the cycloaddition of 1-hex-4-enyl radical was much larger for the endo-cycloaddition, forming a six-member ring, than that for the exo-cycloaddition, forming a five-member ring; this is in contrast to the Baldwin rule.[34] Recently, Wang et al.[35] investigated a series of vinyl migration reactions that proceed though these endo- and exo-cyclic radical intermediates. Their results show that the exo-cyclization reactions that proceed via a three-membered ring are more facile than the endo-cyclization reactions as well as the other exo-cyclization reactions that form larger rings. Sirjean et al.[33] performed a theoretical study of the ring opening β-scission reactions of C_3-C_7 cycloalkyl and methyl cycloalkyl radicals. Their results shows that the activation energy for the endo-ring opening are greater than these of exo-ring opening; similar trends are expected for the reverse reactions.

Scheme 1. Schematic for the 1,4-Endo- and Exo-cycloaddition Reactions

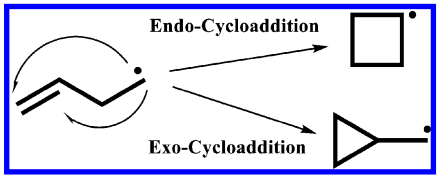

In this study we present electronic structure calculations at the CBS-QB3 level of theory combined with transition state theory to calculate high pressure rate constants for systematic sets of reactions within these two reaction classes. For the H atom shift reactions of alkyl radicals, we investigate the 1,2- through 1,7-H shifts. For the alkenyl radical cycloaddition reactions, we investigate both the endo- and exo-ring closures that lead to the formation of three- to seven-member cycloalkyl radicals. These rate constants serve as the basis for development of high-pressure rate rules. As discussed above, these results are interpreted in the context of structure−reactivity relationships to gain insights into the trends of the activation and ring strain energies as well as in the pre-exponential factors. The impact of ring size and substituent effects are investigated. This is the first in a series of two papers; the second paper examines the impact of resonant stabilization on these reaction types.

METHODS

Electronic structure calculations were carried out using the Gaussian 03 and 09 suites of programs.[36,37] The CBS-QB3 composite method[38] was used to calculate optimized geometries, frequencies, and electronic energies for the lowest energy conformer of the reactants, products, and transition states. This method has been shown to predict heats of formation for a large test set of molecules with an accuracy of just over 1 kcal/mol.[38] Low frequency vibrational modes that resemble torsions around single bonds were treated as hindered internal rotors rather than as harmonic oscillators. Hindrance potentials were calculated at the B3LYP/6-31G(d) level of theory via relaxed surface scans with a step size of 10°. Hindered potentials (with barriers $\leq$ 12 kcal/mol) were fit to truncated Fourier series expansions. Reduced moments of inertia for asymmetric internal rotors were calculated at the I(2,3) level based on the equilibrium geometry as defined by East and Radom.[39] The 1-D Schrödinger equation was numerically solved for each internal rotor using the eigenfunctions of the 1-D free rotor as basis functions. The energy eigenvalues are then used to numerically calculate their contributions to thermodynamic functions. All other modes were treated as harmonic oscillators, and the frequencies were scaled by a factor of 0.99. Thermodynamic properties (e.g., $\Delta_f H_{298}$, S_{298}, and C_p values) were calculated using standard statistical mechanics methods. The electronic energy of each species was converted to its heat of formation using the atomization method. Since only relative energies are required in this work, no attempts were made to improve the heats of formation using, for example, bond additivity corrections. Inspections of the hindered rotor potentials help ensure that the optimized geometry of a molecule corresponds to the lowest energy minimum. A normal-mode analysis was performed to identify the nature of the species. Transition states were identified by having one imaginary frequency, which was animated to verify that it corresponds to the desired reaction coordinate. A more detailed description can be found in earlier publications.[40−42]

High-pressure rate coefficients were calculated using canonical transition state theory (TST): $k(T) = \kappa(T)\cdot k_B T/h\cdot$

DOI: 10.1021/jp511017z
J. Phys. Chem. A XXXX, XXX, XXX−XXX

$\exp(-\Delta G^{\ddagger}/RT)$, where $\kappa(T)$ is the tunneling correction factor, and $\Delta G^{\ddagger}$ is the Gibbs free energy difference between the transition state, minus the contribution from the reaction coordinate, and the reactants. The remaining variables have their usual meaning. Tunneling correction factors were calculated with an asymmetric Eckart potential.[43] Previous studies on H atom shift reactions have shown that this method can accurately predict the tunneling correction factors.[5] Rate constants were calculated over a temperature range of 300−2500 K in 50 K increments and fit to modified Arrhenius expressions: $k(T) = A'\cdot T^{n}\cdot\exp(-E/RT)$. The estimated uncertainty in the calculated rate coefficients is roughly a factor of 3 near 1000 K. Uncertainties arise from errors in the ab initio method such as variations in optimized reactant and TS geometries as well as errors in the harmonic frequencies and hindered rotor calculations.

Several identity H atom shift reactions were evaluated (i.e., the reactant and the product are identical). Since the corresponding transition states are symmetric with respect to the reaction coordinate, the pre-exponential factors are multiplied by a factor of 2 to account for the fact that passage though the transition state from either direction (the reactant or product) results in an indistinguishable H-shift, which doubles the rate constant.[44,45] Another scenario arises for cases where substituents are present in the transition state ring structure; this results in the presence of two or more isomers. In many cases, in planar transition state ring structures (e.g., the 1,2- to 1,4 H atom shift transition states), these are optical isomers, and the entropies are corrected by adding $R\cdot\ln(2)$, which increases the rate constant by a factor of 2. However, if two or more substituents are present at different locations on the ring or if the ring is nonplanar, these isomers are energetically distinct. Both the axial and equatorial structures were calculated, leading to two or more rate constants, which were then summed to get a total value.

The individual rate coefficients serve as the basis to develop the rate rule for a given reaction subclass. For a given subclass of reactions, the rate rule was obtained by averaging the rate coefficients for each reaction at each temperature and then fitting these averages to a modified Arrhenius expression. The rate rules were also fit to a simple Arrhenius form over a narrower range of 500−1500 K or at specific temperature (e.g., 298 K) to provide a framework to connect the parameters more directly to a physical picture of the reaction, i.e., the impact of losing internal rotors on the pre-exponential factor and the impact of ring size on ring strain. The simplified Arrhenius rate parameters are determined from $E_a = E + nRT$ and $A = k(T)/\exp(-(E + nRT)/RT))$, where the n and E parameters are taken from the modified Arrhenius fits.

In several places throughout the text, tables, and figures, we employ a chemical notation that omits the hydrogen atoms. A radical site is indicated by a bullet and a double bond by an equal sign. The units employed are kcal, sec, and mol.

RESULTS

H-Shift Reactions of Alkyl Radicals. Table 1 presents the results for the 1,2- through 1,7-H atom shift reactions. The following notation is used: For a 1,x-H shift, x refers to the location of the carbon from which the hydrogen is abstracted relative to the carbon of the original radical site. Thus, a 1,2-shift proceeds through a three-member ring transition state and so forth. The rate constants are listed in a modified Arrhenius form and the pre-exponential factors are normalized to reflect the number of degenerate hydrogen atoms. For these reactions, the value "n" in the modified Arrhenius fits ranges from ∼1.3 to ∼2.2. Although this is smaller than the typical values of ∼3 for bimolecular hydrogen abstractions, it does indicate significant upward curvature on an Arrhenius plot. Thus, use of the modified Arrhenius form is essential to properly describe the temperature dependence over a wide range. For substituted H atom shift reactions that can proceed via axial and equatorial transition state structures, the reported rate parameters are obtained by fitting the sum of two or more rate constants. Typically, the equatorial transition state is lower in energy than the axial one.

The rate constants for these isomerization reactions group together according to the size of ring formed in the transition state. Figure 1 compares the rate constants for the simplest n-alkyl radical in each one of the categories. The pre-exponential factors decrease as the size of the ring increases. The activation energies also decrease in going from a three- and four-member ring to a five-member ring, then again to a six- and seven-member ring, before slightly increasing with the formation of an eight-member ring. These trends will be discussed in detail later in the text.

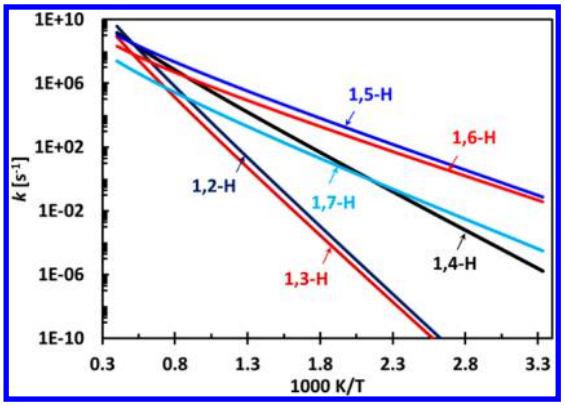

Figure 1. Comparison of rate constants for n-alkyl radical isomerization for the simplest H-shift in each reaction category.

Within each ring-size category, there are six further subcategories depending upon the nature of the radical site and the abstracted hydrogen atom. These include primary−primary (i.e., a primary radical forming another primary radical after the H-shift, which is abbreviated to pp), secondary−secondary (ss), tertiary−tertiary (tt), secondary−tertiary (st), primary−secondary (ps), and primary−tertiary (pt). Of these, the pp, ss, and tt reaction types are very close to thermoneutral. For the other three reaction types, the reaction enthalpy increases in going from st to ps to pt. Although it is somewhat challenging to see in the modified Arrhenius form, the energy barriers correlate with the reaction enthalpies. Thus, for a given type of radical, the barrier deceases with increasing substation (e.g., pp > ps > pt and ss > st). Interestingly, however, the barriers also decrease with increasing substitution within the group of thermoneutral reactions (e.g, pp > ss > tt). Due to these differences, we have assigned six rate rules for each ring-size category. The rate rules for the 1,5-H shift reactions are shown in Figure 2; the rate rules for all the 1,x-shifts are provided in the Supporting Information, Figure S1.

For most of the cases, we have evaluated enough reactions within each subcategory to enable the development of six rules for each category of H atom shift. For some of the larger-sized

DOI: 10.1021/jp511017z
J. Phys. Chem. A XXXX, XXX, XXX−XXX

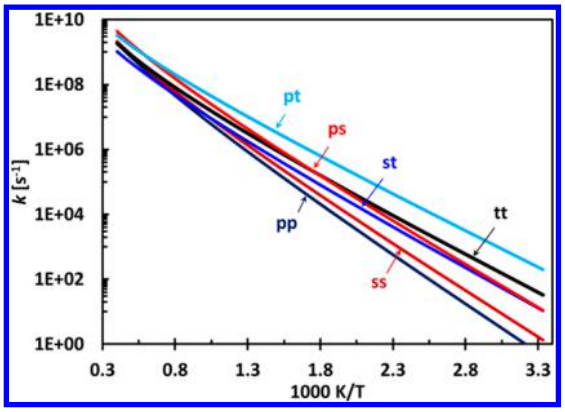

Figure 2. Comparison of rate constant rules for different reaction subcategories for a 1,5-H shift.

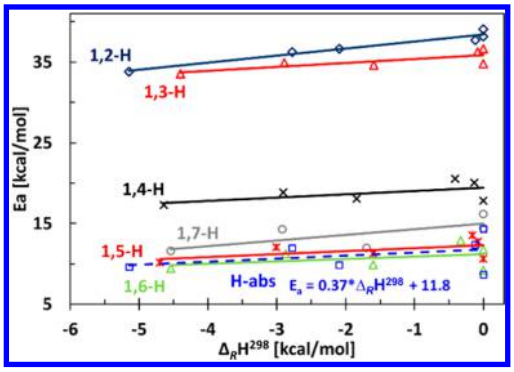

Figure 3. Evans–Polanyi relationships for the 1,2- to 1,7-H shift isomerization at 298 K.

species, only one or two reactions were evaluated in each subcategory. In these cases, the rate parameters are consistent with the trends observed for the whole set of H atom shift reactions. The overall consistency of the activation energies is evident in the Evans–Polanyi relationships shown in Figure 3. Also provided in Table 1 are the ratios of the TST-derived rate constant at 500 and 1500 K to that obtained from the rate estimation rule. In most cases, this ratio is within a factor of 2. However, there are some exceptions; in several instances, it is observed that the simplest reactions within a given subcategory have the smallest rate constants (e.g., reactions 25, 55, and 67 are lower than the rate rule). This is generally due to the slightly higher activation energy (~0.6–1.3 kcal/mol).

The impact of substitution has previously been investigated. Davis and Francisco[4,27] performed a comprehensive investigation on the effect of methyl substitution at various positions along the backbone of 1-alkyl radicals. Consistent with previous findings,[2,3,25] their results show that the activation energy decreases as the degree of branching around the abstracted C–H site increases, reflecting the changes in the enthalpy of reaction, e.g., $k_{pp} < k_{ps} < k_{pt}$. Interestingly, the addition of methyl groups at other carbon sites along the alkyl chain also tends to lower the activation energy (by ~0.8 to 1.6 kcal/mol). This is attributed to the presence of gauche interactions in the reactant that are partially relieved in the transition state structure. While we do not provide a systematic investigation, we do provide several examples that show the impact of substitution. The results presented here are consistent with those of Davis and Francisco,[4] and we further show that the presence of additional or larger groups will lower the activation energy even more. Despite this, however, the majority of the rate constants still fall within a factor of 2 of the rate rules. This is because there are also changes in the pre-exponential factor that often offset the decrease in barrier height.

Several prior experimental and theoretical studies have been conducted for the H atom shift reactions. Sirjean et al.[5] has provided a review of the available experimental values, the majority of which are on the 1,4- and 1,5-H shift reactions, and they calculated several cases using CBS-QB3 calculations. Figure 4 compares the results of the present work to that of Sirjean et al.[5] as well as to experimental measurements for the 1,4-H atom shift of *n*-pentyl and 1,6-H shift in *n*-hexyl. The two CBS-QB3 derived values are in reasonable agreement, especially when one considers the various approaches to account for hindered rotors.[46] Furthermore, both sets of calculated values are in good agreement with the experimental data. Additional comparisons are provided in the Supporting Information in Figure S2.

Cycloaddition Reactions of Alkenyl Radicals. There are two available sites for intramolecular addition to the double bond of alkenyl radicals: the endo- and the exo-positions. The following notation is used: For a 1,*x*-cycloaddition, *x* refers to the location of the carbon radical relative to the far vinylic

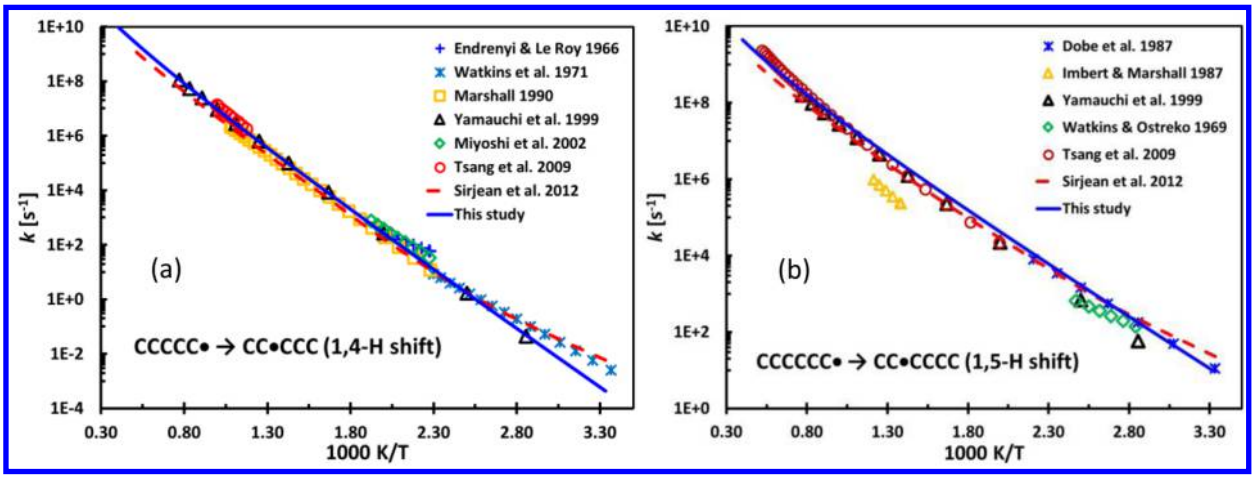

Figure 4. Comparisons of the CBS-QB3 rate constants calculated in this study for (a) CCCCC• → CC•CCC and (b) CCCCCC• → CC•CCCC to those available in the literature.

DOI: 10.1021/jp511017z
J. Phys. Chem. A XXXX, XXX, XXX–XXX

Table 1. Calculated Rate Parameters, Rate Constants, and Heats of Reactions for the H-Shift Isomerization Reactions[a,b,c]

#	reactions	n_H	modified Arrhenius parameters A_H	n	E	$\Delta_R H^{298}$ [kcal/mol]	k_{TST} (k_{rule}/k_{TST}) on a per H basis 500 K		1500 K	
	1,2-H shift									
	pp									
1	$C_2H_5 \rightarrow C_2H_5$	3	4.71×10^{06}	1.81	37.1	0	1.93×10^{-05}		1.11×10^{07}	
	ss rate rule		$\mathbf{4.02 \times 10^{06}}$	**1.86**	**36.6**	**−0.1**	$\mathbf{4.06 \times 10^{-05}}$		$\mathbf{1.52 \times 10^{07}}$	
2	CCC•C → CCC•C	2	5.85×10^{06}	1.83	36.8	0	3.76×10^{-05}	1.08	1.77×10^{07}	0.86
3	CCCC•CC → CCCC•CC	2	3.35×10^{06}	1.91	36.5	0	4.47×10^{-05}	0.91	1.91×10^{07}	0.80
4	CCCCC•C → CCCC•CC	2	3.09×10^{06}	1.88	36.6	−0.17	3.25×10^{-05}	1.25	1.45×10^{07}	1.05
5	CCCC•C → CCC•CC	2	4.69×10^{06}	1.82	36.7	−0.31	3.09×10^{-05}	1.31	1.37×10^{07}	1.11
	tt									
6	$C_2C•CC_2 \rightarrow C_2C•CC_2$	1	8.38×10^{07}	1.60	38.1	0	3.28×10^{-05}		2.93×10^{07}	
	st rate rule		$\mathbf{5.74 \times 10^{07}}$	**1.53**	**35.7**	**−2.10**	$\mathbf{1.77 \times 10^{-04}}$		$\mathbf{2.49 \times 10^{07}}$	
7	$C_2CC•C \rightarrow CCC•C_2$	1	1.22×10^{08}	1.45	36.0	−1.95	1.64×10^{-04}	1.08	2.83×10^{07}	0.88
8	$C_2CC•CC \rightarrow CCCC•C_2$	1	2.92×10^{07}	1.60	35.5	−2.24	1.64×10^{-04}	1.08	2.40×10^{07}	1.04
	ps rate rule		$\mathbf{3.24 \times 10^{07}}$	**1.57**	**35.3**	**−2.86**	$\mathbf{2.02 \times 10^{-04}}$		$\mathbf{2.29 \times 10^{07}}$	
9	$C_2CCC• \rightarrow C_2CC•C$	2	3.18×10^{07}	1.61	35.5	−2.45	1.92×10^{-04}	1.05	3.00×10^{07}	0.76
10	CCCC• → CCC•C	2	2.07×10^{07}	1.64	35.4	−2.81	1.72×10^{-04}	1.18	2.49×10^{07}	0.92
11	CCCCC• → CCCC•C	2	2.42×10^{07}	1.62	35.2	−2.96	2.04×10^{-04}	0.99	2.59×10^{07}	0.88
12	CCCCCC• → CCCCC•C	2	2.46×10^{07}	1.61	35.2	−2.97	2.00×10^{-04}	1.01	2.52×10^{07}	0.91
13	CCC• → CC•C	2	2.36×10^{07}	1.62	35.2	−3.15	2.15×10^{-04}	0.94	2.64×10^{07}	0.87
14	$C{=}C_2CC• \rightarrow C{=}C_2CC•C$	2	5.60×10^{06}	1.80	35.1	−2.91	1.64×10^{-04}	1.23	2.34×10^{07}	0.98
15	$C{=}CC_2CC• \rightarrow C{=}CC_2C•C$	2	4.05×10^{06}	1.85	35.1	−2.62	1.59×10^{-04}	1.28	2.41×10^{07}	0.95
16	C=CCCCC• → C=CCCC•C	2	2.41×10^{07}	1.63	35.4	−2.84	1.84×10^{-04}	1.10	2.68×10^{07}	0.86
17	trans-CC=CCCC• → trans-CC=CCC•C	2	2.22×10^{06}	1.91	35.3	−2.54	1.06×10^{-04}	1.91	1.85×10^{07}	1.24
18	cis-CC=CCCC• → cis-CC=CCC•C	2	1.61×10^{07}	1.65	35.7	−2.52	1.02×10^{-04}	1.98	1.90×10^{07}	1.21
19	C•Ccy(CCCC) → CC•cy(CCCC)	2	2.35×10^{07}	1.61	34.8	−3.65	2.99×10^{-04}	0.68	2.79×10^{07}	0.82
	pt rate rule		$\mathbf{1.51 \times 10^{08}}$	**1.39**	**33.0**	**−5.48**	$\mathbf{3.27 \times 10^{-03}}$		$\mathbf{6.23 \times 10^{07}}$	
21	$C_2CC• \rightarrow C_3C•$	1	7.92×10^{07}	1.48	33.2	−5.10	2.20×10^{-03}	1.48	5.88×10^{07}	1.06
22	$CCCC_2• \rightarrow CCC•C_2$	1	2.88×10^{08}	1.32	33.1	−5.15	3.23×10^{-03}	1.01	6.77×10^{07}	0.92
23	$C{=}CCCC_2• \rightarrow C{=}CCC•C_2$	1	1.30×10^{08}	1.43	33.2	−5.19	2.50×10^{-03}	1.31	6.64×10^{07}	0.94
24	$C_2•Ccy(CCC) \rightarrow C_2C•cy(CCC)$	1	3.72×10^{08}	1.27	32.8	−6.49	4.26×10^{-03}	0.77	6.73×10^{07}	0.93
	1,3-H shift									
	pp rate rule		$\mathbf{5.90 \times 10^{04}}$	**2.17**	**35.4**	**0.00**	$\mathbf{1.39 \times 10^{-05}}$		$\mathbf{3.15 \times 10^{06}}$	
25	CCC• → CCC•	3	6.87×10^{04}	2.13	36.1	0	5.77×10^{-06}	2.41	2.29×10^{06}	1.37
26	$C_2CC• \rightarrow CCC_2•$	6	1.10×10^{05}	2.11	35.8	0	1.09×10^{-05}	1.28	3.37×10^{06}	0.94
27	$C_3CC• \rightarrow C_3CC•$	9	1.43×10^{05}	2.07	35.1	0	2.23×10^{-05}	0.62	4.27×10^{06}	0.74
	ss rate rule		$\mathbf{1.11 \times 10^{05}}$	**2.16**	**35.1**	**−0.09**	$\mathbf{3.43 \times 10^{-05}}$		$\mathbf{6.19 \times 10^{06}}$	
28	CCCC•C → CCCC•C	2	1.80×10^{05}	2.12	35.4	0	3.05×10^{-05}	1.12	7.25×10^{06}	0.85
29	CCCC•CC → CCCCC•C	2	9.34×10^{04}	2.16	34.8	−0.17	3.30×10^{-05}	1.04	5.80×10^{06}	1.07
	tt									
30	$C_2C•CCC_2 \rightarrow C_2CCC•C_2$	1	2.54×10^{05}	2.03	33.6	0.00	1.46×10^{-04}		9.76×10^{06}	
	st									
31	$C_2CCC•C \rightarrow C_2C•CCC$	1	7.12×10^{05}	1.82	33.6	−1.59	1.16×10^{-04}		5.87×10^{06}	
	ps rate rule		$\mathbf{5.32 \times 10^{05}}$	**1.93**	**33.8**	**−2.79**	$\mathbf{1.46 \times 10^{-04}}$		$\mathbf{8.73 \times 10^{06}}$	
32	CCCCC• → CCC•CC	2	4.38×10^{05}	1.98	34.1	−2.64	1.14×10^{-04}	1.29	9.50×10^{06}	0.92
33	CCCC• → CCC•C	2	4.07×10^{05}	1.97	34.4	−2.81	7.35×10^{-05}	1.99	7.55×10^{06}	1.16
34	CCCCCC• → CCCC•CC	2	3.76×10^{05}	1.96	33.9	−2.81	1.02×10^{-04}	1.44	7.55×10^{06}	1.16
35	C=CCCCC• → C=CCC•CC	2	1.11×10^{05}	2.11	34.0	−2.33	6.70×10^{-05}	2.18	6.50×10^{06}	1.34
36	C=CC(C•)CC → C=CC(C)C•C	2	7.55×10^{06}	1.62	33.8	−2.96	2.85×10^{-04}	0.51	1.26×10^{07}	0.69
37	$CCCC_2• \rightarrow C_2CC•C$	2	8.78×10^{05}	1.88	33.7	−3.20	1.91×10^{-04}	0.77	1.08×10^{07}	0.81
	pt									
38	$C_2CCC• \rightarrow CCC•C_2$	1	1.73×10^{06}	1.79	32.5	−4.40	6.42×10^{-04}		1.52×10^{07}	
	1,4-H shift									
	pp rate rule		$\mathbf{7.59 \times 10^{04}}$	**1.74**	**19.8**	**−0.37**	$\mathbf{8.37 \times 10^{00}}$		$\mathbf{3.25 \times 10^{07}}$	
39	CCCC• → CCCC•	3	1.29×10^{05}	1.73	20.8	0	4.70×10^{00}	1.78	3.71×10^{07}	0.88
40	C=CC(C•)CC → C=CC(C)CC•	3	5.05×10^{05}	1.47	19.7	−0.34	1.16×10^{01}	0.72	3.08×10^{07}	1.06
41	$CCCC_2• \rightarrow C_2CCC•$	3	2.05×10^{05}	1.59	19.7	−0.76	9.37×10^{00}	0.89	2.97×10^{07}	1.10
	ss rate rule		$\mathbf{3.87 \times 10^{05}}$	**1.66**	**19.1**	**−0.13**	$\mathbf{5.10 \times 10^{01}}$		$\mathbf{1.20 \times 10^{08}}$	
42	CC•CCCC → CCCCC•C	2	5.94×10^{05}	1.66	19.5	0	5.44×10^{01}	0.94	1.58×10^{08}	0.76
43	CC•CCCCC → CCCCC•CC	2	6.18×10^{05}	1.59	19.1	−0.04	5.51×10^{01}	0.93	1.13×10^{08}	1.06
44	CCCC•CCCC → CCCCCCC•C	2	2.58×10^{05}	1.67	18.9	−0.35	4.52×10^{01}	1.13	9.08×10^{07}	1.32

DOI: 10.1021/jp511017z
J. Phys. Chem. A XXXX, XXX, XXX−XXX

Table 1. continued

#	reactions	n_H	modified Arrhenius parameters A_H	n	E	$\Delta_R H^{298}$ [kcal/mol]	k_{TST} (k_{rule}/k_{TST}) on a per H basis 500 K		1500 K	
	1,4-H shift									
	tt									
45	$C_2C^{\bullet}CCCC_2 \rightarrow C_2CCCC^{\bullet}C_2$	1	7.48×10^{04}	1.81	16.8	0	2.64×10^{02}		1.52×10^{08}	
	st									
46	$C_3CCC^{\bullet}C \rightarrow C_3{}^{\bullet}CCCC$	1	5.02×10^{05}	1.52	17.2	−1.84	1.98×10^{02}		1.07×10^{08}	
	ps rate rule		$\mathbf{3.77 \times 10^{05}}$	**1.63**	**17.9**	**−2.91**	$\mathbf{1.38 \times 10^{02}}$		$\mathbf{1.37 \times 10^{08}}$	
47	$C^{\bullet}CCCCCCC \rightarrow CCCC^{\bullet}CCCC$	2	1.26×10^{06}	1.51	18.2	−2.58	1.72×10^{02}	0.80	1.79×10^{08}	0.77
48	$C_3CCCC^{\bullet} \rightarrow C_3C^{\bullet}CCC$	2	9.12×10^{05}	1.54	18.1	−2.60	1.64×10^{02}	0.84	1.61×10^{08}	0.85
49	$CCC_2CC^{\bullet} \rightarrow CC^{\bullet}C_2CC$	2	3.43×10^{05}	1.56	17.6	−2.72	1.10×10^{02}	1.25	8.09×10^{07}	1.69
50	$C^{\bullet}CCCCC \rightarrow CCC^{\bullet}CCC$	2	1.18×10^{06}	1.52	18.4	−2.81	1.35×10^{02}	1.02	1.63×10^{08}	0.84
51	$C^{\bullet}CCCCCC \rightarrow CCCC^{\bullet}CCC$	2	8.05×10^{05}	1.53	18.2	−2.88	1.16×10^{02}	1.19	1.25×10^{08}	1.10
52	$CCCCC^{\bullet} \rightarrow CCCC^{\bullet}C$	2	1.15×10^{06}	1.51	18.6	−2.96	9.75×10^{01}	1.41	1.33×10^{08}	1.03
53	$C^{\bullet}C_2CCC \rightarrow CC_2CC^{\bullet}C$	2	2.76×10^{06}	1.39	17.6	−3.80	3.24×10^{02}	0.42	1.98×10^{08}	0.69
	pt									
54	$C_3CCC^{\bullet} \rightarrow C_3{}^{\bullet}CCC$	1	3.35×10^{06}	1.39	16.5	−4.64	1.18×10^{03}		3.31×10^{08}	
	1,5-H shift									
	pp rate rule		$\mathbf{4.59 \times 10^{04}}$	**1.68**	**12.6**	**−0.16**	$\mathbf{4.89 \times 10^{03}}$		$\mathbf{1.46 \times 10^{08}}$	
55	$CCCCC^{\bullet} \rightarrow CCCCC^{\bullet}$	3	3.17×10^{04}	1.67	13.4	0	1.51×10^{03}	3.23	7.07×10^{07}	2.07
56	$CCC_2CC^{\bullet} \rightarrow CCC_2CC^{\bullet}$	3	5.22×10^{04}	1.70	12.6	0	6.67×10^{03}	0.73	1.86×10^{08}	0.79
57	$C^{\bullet}C_2CCC \rightarrow CC_2CCC^{\bullet}$	3	1.15×10^{05}	1.58	12.5	−0.48	7.33×10^{03}	0.67	1.73×10^{08}	0.85
	ss rate rule		$\mathbf{6.37 \times 10^{04}}$	**1.64**	**12.0**	**−0.08**	$\mathbf{9.74 \times 10^{03}}$		$\mathbf{1.85 \times 10^{08}}$	
58	$CC^{\bullet}CCCCC \rightarrow CCCCCC^{\bullet}C$	2	1.11×10^{05}	1.53	12.3	0	1.29×10^{04}	0.76	2.50×10^{08}	0.74
59	$CCC^{\bullet}CCCCC \rightarrow CCCCCCC^{\bullet}C$	2	1.15×10^{04}	1.79	11.5	−0.16	7.66×10^{03}	1.27	1.14×10^{08}	1.62
	tt									
60	$C_2C^{\bullet}CCCCC_2 \rightarrow C_2CCCCC^{\bullet}C_2$	1	1.69×10^{04}	1.73	9.6	0	5.24×10^{04}		2.10×10^{08}	
61	$C_3CCCC^{\bullet}C \rightarrow C_3{}^{\bullet}CCCCC$	1	1.53×10^{05}	1.40	10.5	−1.60	2.59×10^{04}		1.23×10^{08}	
	ps rate rule		$\mathbf{1.31 \times 10^{05}}$	**1.62**	**11.1**	**−3.01**	$\mathbf{4.30 \times 10^{04}}$		$\mathbf{4.34 \times 10^{08}}$	
62	$C^{\bullet}CCCCCCC \rightarrow CCCC^{\bullet}CCCC$	2	9.73×10^{04}	1.63	11.0	−2.58	4.11×10^{04}	1.05	3.67×10^{08}	1.18
63	$C^{\bullet}CCCCC \rightarrow CCCCC^{\bullet}C$	2	2.50×10^{05}	1.46	11.5	−2.92	2.25×10^{04}	1.91	2.22×10^{08}	1.96
64	$C^{\bullet}CCCCCC \rightarrow CCCCC^{\bullet}CC$	2	1.18×10^{05}	1.55	11.1	−3.02	2.69×10^{04}	1.60	2.48×10^{08}	1.75
65	$C^{\bullet}C_2CCCC \rightarrow CC_2CCC^{\bullet}C$	2	3.44×10^{05}	1.37	10.5	−3.52	4.69×10^{04}	0.92	2.22×10^{08}	1.96
	pt									
66	$C_3CCCC^{\bullet} \rightarrow C_3{}^{\bullet}CCCC$	1	1.03×10^{06}	1.27	9.4	−4.70	2.31×10^{05}		4.71×10^{08}	
	1,6-H shift									
	pp rate rule		$\mathbf{2.46 \times 10^{03}}$	**1.79**	**11.9**	**−0.33**	$\mathbf{1.05 \times 10^{03}}$		$\mathbf{2.21 \times 10^{07}}$	
67	$C^{\bullet}CCCCC \rightarrow CCCCCC^{\bullet}$	3	2.45×10^{03}	1.78	12.7	0	5.01×10^{02}	2.11	1.53×10^{07}	1.45
68	$C^{\bullet}C_2CCCC \rightarrow CC_2CCCC^{\bullet}$	3	6.38×10^{03}	1.69	11.8	−0.66	1.80×10^{03}	0.59	2.73×10^{07}	0.81
	ss									
69	$CC^{\bullet}CCCCCC \rightarrow CCCCCCC^{\bullet}C$	2	6.71×10^{03}	1.75	10.7	0	7.71×10^{03}		6.37×10^{07}	
70	$C_2C^{\bullet}CCCCC_2 \rightarrow C_2CCCCCC^{\bullet}C_2$	1	1.54×10^{03}	1.78	8.2	0	2.80×10^{04}		4.28×10^{07}	
71	$C_3CCCCC^{\bullet}C \rightarrow C_3{}^{\bullet}CCCCCC$	1	1.65×10^{04}	1.50	9.0	−1.60	2.40×10^{04}		4.62×10^{07}	
	ps rate rule		$\mathbf{1.29 \times 10^{04}}$	**1.67**	**10.2**	**−2.88**	$\mathbf{1.39 \times 10^{04}}$		$\mathbf{8.45 \times 10^{07}}$	
72	$C^{\bullet}CCCCCC \rightarrow CCCCCC^{\bullet}C$	2	2.51×10^{04}	1.64	10.5	−2.98	1.24×10^{04}	1.12	8.43×10^{07}	1.00
73	$C^{\bullet}CCCCCCC \rightarrow CCCCCC^{\bullet}CC$	2	1.43×10^{04}	1.64	10.0	−2.77	1.78×10^{04}	0.78	7.94×10^{07}	1.06
	pt									
74	$C_3CCCCC^{\bullet} \rightarrow C_3{}^{\bullet}CCCCCC$	1	5.15×10^{04}	1.35	8.6	−4.54	4.07×10^{04}		5.10×10^{07}	
	1,7-H shift									
	pp rate rule		$\mathbf{4.28 \times 10^{01}}$	**2.10**	**15.1**	**−0.37**	$\mathbf{1.39 \times 10^{04}}$		$\mathbf{8.45 \times 10^{07}}$	
75	$C^{\bullet}CCCCCC \rightarrow CCCCCCC$	3	1.00×10^{02}	1.99	15.7	0	3.65×10^{00}	1.35	1.06×10^{06}	1.18
76	$CCCCCCC_2^{\bullet} \rightarrow C^{\bullet}CCCCC_2$	3	5.62×10^{01}	2.07	14.9	−0.73	6.53×10^{00}	0.75	1.41×10^{06}	0.89
	ss									
77	$CC^{\bullet}CCCCCCC \rightarrow CCCCCCCC^{\bullet}C$	2	9.92×10^{01}	2.00	13.2	0	4.55×10^{01}		2.53×10^{06}	
78	$C_3CCCCC^{\bullet}C \rightarrow C_3{}^{\bullet}CCCCCCCC$	1	1.93×10^{02}	1.74	11.0	−1.70	1.66×10^{02}		1.51×10^{06}	
	ps									
79	$C^{\bullet}CCCCCCC \rightarrow CCCCCCC^{\bullet}C$	2	5.31×10^{02}	1.81	13.2	−2.92	7.60×10^{01}		3.33×10^{06}	
	pt									
80	$C_3CCCCCC^{\bullet} \rightarrow C_3{}^{\bullet}CCCCCCC$	1	1.55×10^{03}	1.61	10.7	−5.08	8.20×10^{02}		5.20×10^{06}	

[a]The units for A_H, A'_H and k_{TST}, k_{rule} are s^{-1}, and are kcal/mol for E; the A terms are normalized by the number of equivalent hydrogens. [b]The k(rate rule) term has been calculated using the bold rate rule listed for each subset. [c]Molecule structures are presented in abbreviated form (H atoms missing, radical site marked with "•") to improve readability. For example, $C{=}CC_2$ represents isobutene.

DOI: 10.1021/jp511017z
J. Phys. Chem. A XXXX, XXX, XXX−XXX

Table 2. Calculated Rate Parameters, Rate Constants, and Heats of Reactions for the Endo-cycloaddition Reactions for Alkenyl Radicals[a,b,c]

#	reaction reactants	modified Arrhenius parameters			$\Delta_R H^{298}$ [kcal/mol]	k_{TST} (k_{rule}/k_{TST})			
		A	n	E		500 K		1500 K	
	1,4-endo-cycloaddition	**6.34 × 10^{07}**	**1.12**	**29.5**	**3.9**	**8.40 × 10^{-03}**		**1.13 × 10^{07}**	
1	C═CCC$^{\bullet}$	6.60 × 10^{07}	1.08	30.4	4.6	2.87 × 10^{-03}	2.9	6.84 × 10^{06}	1.6
2	C═CCC$^{\bullet}$C	1.02 × 10^{07}	1.34	30.1	4.9	2.88 × 10^{-03}	2.9	7.86 × 10^{06}	1.4
3	C═CCC$^{\bullet}$CC	1.00 × 10^{07}	1.34	29.4	4.2	5.58 × 10^{-03}	1.5	9.52 × 10^{06}	1.2
4	trans-CC═CCC$^{\bullet}$	1.61 × 10^{08}	0.96	29.4	4.7	9.33 × 10^{-03}	0.9	9.62 × 10^{06}	1.2
5	cis-CC═CCC$^{\bullet}$ *	4.74 × 10^{06}	1.37	32.1	3.5	2.18 × 10^{-04}		2.25 × 10^{06}	
6	C═CCC$_2^{\bullet}$	2.01 × 10^{08}	1.02	29.7	3.6	1.19 × 10^{-02}	0.7	1.62 × 10^{07}	0.7
7	C═C$_2$CC$^{\bullet}$	3.82 × 10^{08}	0.91	30.0	3.2	8.11 × 10^{-03}	1.0	1.23 × 10^{07}	0.9
8	C═CCC$_3^{\bullet}$	2.41 × 10^{08}	0.96	29.3	2.8	1.46 × 10^{-02}	0.6	1.48 × 10^{07}	0.8
9	C═CCC$^{\bullet}$C$_2$	2.02 × 10^{06}	1.58	29.7	4.8	3.48 × 10^{-03}	2.4	9.60 × 10^{06}	1.2
10	C═C$_2$CC$^{\bullet}$C	2.71 × 10^{08}	0.99	29.7	3.4	1.33 × 10^{-02}	0.6	1.73 × 10^{07}	0.7
11	C$_2$C═CCC$^{\bullet}$ *	1.15 × 10^{07}	1.24	30.9	3.7	7.50 × 10^{-04}		3.02 × 10^{06}	
	1,5-endo-cycloaddition	**9.87 × 10^{06}**	**1.06**	**13.0**	**−18.7**	**1.56 × 10^{04}**		**3.02 × 10^{08}**	
12	C═CCCC$^{\bullet}$	1.65 × 10^{07}	1.02	14.2	−18.5	1.41 × 10^{04}	1.1	5.08 × 10^{08}	0.6
13	C═CCCC$^{\bullet}$C	4.64 × 10^{06}	1.15	13.9	−18.0	5.31 × 10^{03}	2.9	1.95 × 10^{08}	1.6
14	C═CCCC$^{\bullet}$C$_2$	1.07 × 10^{06}	1.38	12.2	−17.9	2.54 × 10^{04}	0.6	4.18 × 10^{08}	0.7
15	cis-CC═CCCC$^{\bullet}$	5.66 × 10^{06}	1.13	15.9	−19.1	7.19 × 10^{02}		1.05 × 10^{08}	
16	trans-CC═CCCC$^{\bullet}$	2.94 × 10^{07}	0.93	13.9	−17.6	1.63 × 10^{04}	1.0	4.84 × 10^{08}	0.6
17	C═CCCC$_2^{\bullet}$	6.65 × 10^{07}	0.83	13.4	−18.6	1.70 × 10^{04}	0.9	3.20 × 10^{08}	0.9
18	C═CC$_2$CC$^{\bullet}$	7.25 × 10^{07}	0.83	14.1	−19.2	9.48 × 10^{03}	1.6	2.73 × 10^{08}	1.1
19	C═C$_2$CCC$^{\bullet}$	2.23 × 10^{07}	1.00	13.5	−19.3	1.43 × 10^{04}	1.1	3.55 × 10^{08}	0.8
20	C═CCCC$_3^{\bullet}$	1.38 × 10^{08}	0.75	12.6	−19.3	5.05 × 10^{04}	0.3	4.86 × 10^{08}	0.6
21	C═CC(C$_2$)CC$^{\bullet}$	1.60 × 10^{08}	0.76	13.4	−20.0	2.60 × 10^{04}	0.6	4.55 × 10^{08}	0.7
22	C$_2$C═CCCC$^{\bullet}$ *	4.90 × 10^{06}	1.13	15.6	−18.2	8.64 × 10^{02}		9.94 × 10^{07}	
	1,6-endo-cycloaddition	**2.79 × 10^{06}**	**0.96**	**6.0**	**−22.5**	**2.63 × 10^{06}**		**4.28 × 10^{08}**	
23	C═CCCCC$^{\bullet}$	1.25 × 10^{06}	1.08	6.7	−22.1	1.30 × 10^{06}	2.0	3.34 × 10^{08}	1.3
24	C═CCCCC$^{\bullet}$C	4.87 × 10^{05}	1.17	6.3	−21.8	1.34 × 10^{06}	2.0	3.06 × 10^{08}	1.4
25	C═CCCCC$^{\bullet}$C$_2$	3.30 × 10^{04}	1.42	4.7	−21.4	2.08 × 10^{06}	1.3	2.10 × 10^{08}	2.0
26	cis-CC═CCCCC$^{\bullet}$ *	8.16 × 10^{05}	1.06	8.3	−21.4	1.47 × 10^{05}		1.13 × 10^{08}	
27	trans-CC═CCCCC$^{\bullet}$	1.26 × 10^{06}	1.02	6.3	−22.0	1.30 × 10^{06}	2.0	2.49 × 10^{08}	1.7
28	C═CCCCC$_2^{\bullet}$	2.01 × 10^{06}	1.05	5.8	−23.8	4.26 × 10^{06}	0.6	5.99 × 10^{08}	0.7
29	C═CCC$_2$CC$^{\bullet}$	7.32 × 10^{06}	0.84	5.9	−23.2	3.89 × 10^{06}	0.7	4.64 × 10^{08}	0.9
30	C═CC$_2$CCC$^{\bullet}$	1.24 × 10^{07}	0.79	6.2	−22.8	3.44 × 10^{06}	0.8	4.61 × 10^{08}	0.9
31	C═C$_2$CCCC$^{\bullet}$	1.46 × 10^{06}	1.02	6.1	−23.0	1.93 × 10^{06}	1.4	3.15 × 10^{08}	1.4
32	C═CCCCC$_3^{\bullet}$	1.19 × 10^{07}	0.78	6.2	−23.6	3.03 × 10^{06}	0.9	4.08 × 10^{08}	1.0
33	C═CCC(C$_2$)CC$^{\bullet}$	3.50 × 10^{07}	0.70	6.3	−23.1	4.99 × 10^{06}	0.5	6.61 × 10^{08}	0.6
34	C═CC(C$_2$)CCC$^{\bullet}$	5.85 × 10^{07}	0.63	6.3	−23.2	5.61 × 10^{06}	0.5	6.72 × 10^{08}	0.6
35	C$_2$C═CCCCC$^{\bullet}$ *	3.44 × 10^{05}	1.10	7.7	−21.5	1.40 × 10^{05}		7.87 × 10^{07}	
	1,7-endo-cycloaddition	**3.98 × 10^{04}**	**1.27**	**6.2**	**−19.1**	**2.06 × 10^{05}**		**5.46 × 10^{07}**	
36	C═CCCCCC$^{\bullet}$	1.14 × 10^{05}	1.20	6.5	−19.6	3.26 × 10^{05}	0.6	8.19 × 10^{07}	0.7
37	C═CCCCCC$^{\bullet}$C	2.11 × 10^{04}	1.34	6.4	−18.5	1.47 × 10^{05}	1.4	4.11 × 10^{07}	1.3
38	C═CCCCCC$^{\bullet}$C$_2$	5.54 × 10^{02}	1.66	4.9	−18.0	1.27 × 10^{05}	1.6	1.90 × 10^{07}	2.9
39	cis-CC═CCCCCC$^{\bullet}$ *	6.03 × 10^{04}	1.21	8.1	−19.3	3.37 × 10^{04}		2.64 × 10^{07}	
40	trans-CC═CCCCCC$^{\bullet}$	1.10 × 10^{05}	1.18	6.5	−19.8	2.76 × 10^{05}	0.7	6.91 × 10^{07}	0.8
41	C═C$_2$CCCCC$^{\bullet}$	1.85 × 10^{05}	1.07	6.4	−19.7	2.43 × 10^{05}	0.8	5.03 × 10^{07}	1.1
42	C$_2$C═CCCCCC$^{\bullet}$ *	1.22 × 10^{04}	1.36	8.5	−18.9	1.19 × 10^{04}		1.40 × 10^{07}	

[a]The units for A and k_{TST}, k_{rule} are s^{-1}, and are kcal/mol for E. [b]The k(rate rule) term has been calculated using the bold rate rule listed for each subset; The single star * means the reactions are excluded during the rate rule development. [c]The notation for others are the same as Table 1.

carbon. As shown in Scheme 1, a 1,4-endo-addition leads to the formation of a cyclobutyl radical where the unpaired electron is contained within the ring structure. In the 1,4-exo-addition, a cyclopropyl-carbinyl radical is formed, where the unpaired electron is located outside the ring on the alkyl substituent. In Tables 2 and 3 we provide the calculated rate constants for the 1,4- to 1,7-cycloaddition reactions for the two addition sites, respectively. The investigated endo-cycloadditions form four- to seven-member rings; the endo-reaction that forms a three-member ring will be presented in forthcoming work since it involves a resonantly stabilized radical. The investigated exo-addition reactions form three- to six-member rings. These rate constants show less of a non-Arrhenius temperature dependence, with a typical "n" values in the range of 0.4 to 1.8, whereas a typical bimolecular alkyl radical addition reaction has "n" values ranging from ∼2.5 to ∼3.5. For cycloaddition reactions that can proceed via an axial and equatorial transition state structure, we report the

DOI: 10.1021/jp511017z
J. Phys. Chem. A XXXX, XXX, XXX−XXX

Table 3. Calculated Rate Parameters, Rate Constants, and Heats of Reactions for the Exo-cycloaddition Reactions[a,b,c]

#	reactions	modified Arrhenius parameters			$\Delta_R H^{298}$ [kcal/mol]	$k_{TST}(k_{rule}/k_{TST})$			
		A	n	E		500 K		1500 K	
	1,4-exo-cycloaddition	**1.08×10^{07}**	**1.45**	**6.6**	**2.4**	**1.15×10^{08}**		**4.80×10^{10}**	
1	C═C−C−C•	6.32×10^{08}	0.97	8.9	2.5	3.28×10^{07}	3.5	3.77×10^{10}	1.3
2	C═C−C−C•−C	5.56×10^{08}	1.00	9.3	3.1	2.35×10^{07}	4.9	3.74×10^{10}	1.3
3	C═C−C−C•−C_2	2.47×10^{08}	1.11	9.1	4.1	2.49×10^{07}	4.6	3.89×10^{10}	1.2
4	cis-C−C═C−C−C•	9.92×10^{08}	0.95	8.0	1.6	1.16×10^{08}	1.0	6.91×10^{10}	0.7
5	trans-C−C═C−C−C•	1.68×10^{09}	0.84	9.2	2.7	3.10×10^{07}	3.7	3.64×10^{10}	1.3
6	C═C−C−C_2•	1.08×10^{09}	0.90	7.3	1.5	1.82×10^{08}	0.6	6.56×10^{10}	0.7
7	C═C_2−C−C• *	8.52×10^{08}	0.89	10.4	3.3	6.21×10^{06}		1.78×10^{10}	
8	C═C−C−C_3•	1.85×10^{09}	0.75	6.2	1.1	3.90×10^{08}	0.3	5.61×10^{10}	0.9
9	C_2−C═C−C−C•	2.90×10^{09}	0.79	8.5	1.8	7.67×10^{07}	1.5	5.29×10^{10}	0.9
	1,5-exo-cycloaddition	**1.35×10^{06}**	**1.48**	**12.2**	**1.5**	**6.42×10^{04}**		**1.15×10^{09}**	
10	C═C−C−C−C•	2.07×10^{06}	1.46	14.1	2.5	1.23×10^{04}	5.2	7.90×10^{08}	1.5
11	C═C−C−C−C•−C	4.73×10^{06}	1.31	13.1	2.1	3.05×10^{04}	2.1	8.61×10^{08}	1.3
12	C═C−C−C−C•−C_2	1.02×10^{05}	1.80	11.1	2.2	1.01×10^{05}	0.6	1.27×10^{09}	0.9
13	trans-C−C═C−C−C−C•	8.65×10^{06}	1.30	13.8	2.2	2.51×10^{04}	2.6	1.13×10^{09}	1.0
14	cis-C−C═C−C−C-C•	2.69×10^{07}	1.13	13.9	1.1	2.54×10^{04}	2.5	9.86×10^{08}	1.2
15	C═C−C−C−C_2•	6.52×10^{07}	1.00	13.0	1.1	6.69×10^{04}	1.0	1.26×10^{09}	0.9
16	C═C−C_2−C−C•	3.15×10^{07}	1.08	12.7	0.9	6.84×10^{04}	0.9	1.15×10^{09}	1.0
17	C═C_2−C−C−C• *	6.48×10^{06}	1.25	15.0	2.6	3.96×10^{03}		3.79×10^{08}	
18	C═C−C−C−C_3•	6.20×10^{06}	1.30	11.7	0.0	1.50×10^{05}	0.4	1.63×10^{09}	0.7
19	C═C−C(C_2)−C−C•	2.60×10^{07}	1.13	12.4	0.2	1.14×10^{05}	0.6	1.60×10^{09}	0.7
20	C_2−C═C−C−C−C•	5.53×10^{07}	1.02	13.5	1.3	3.78×10^{04}	1.7	1.01×10^{09}	1.1
	1,6-exo-cycloaddition	**1.60×10^{06}**	**1.20**	**3.8**	**−16.4**	**5.96×10^{07}**		**2.89×10^{09}**	
21	C═C−C−C−C−C•	6.98×10^{05}	1.33	4.7	−15.7	2.45×10^{07}	2.4	2.47×10^{09}	1.2
22	C═C−C−C−C−C•−C	1.87×10^{05}	1.48	3.9	−15.5	3.71×10^{07}	1.6	2.54×10^{09}	1.1
23	C═C−C−C−C−C•−C_2	1.26×10^{05}	1.48	3.7	−15.1	3.01×10^{07}	2.0	1.82×10^{09}	1.6
24	trans-C−C═C−C−C−C−C•	1.72×10^{06}	1.20	4.3	−16.1	4.21×10^{07}	1.4	2.74×10^{09}	1.1
25	cis-C−C═C−C−C−C−C•	9.06×10^{06}	1.01	4.8	−17.2	3.86×10^{07}	1.5	2.87×10^{09}	1.0
26	C═C_2−C−C−C−C• *	1.84×10^{05}	1.40	6.2	−15.1	2.22×10^{06}		6.45×10^{08}	
27	C═C−C−C−C−C_2•	1.25×10^{06}	1.22	3.7	−17.1	5.83×10^{07}	1.0	2.72×10^{09}	1.1
28	C═C−C−C_2−C−C•	8.07×10^{06}	1.02	3.9	−16.3	8.86×10^{07}	0.7	3.71×10^{09}	0.8
29	C═C−C_2−C−C−C•	6.75×10^{06}	1.04	4.5	−16.6	4.69×10^{07}	1.3	3.04×10^{09}	0.9
30	C═C−C−C−C−C_3•	7.05×10^{06}	1.03	3.2	−17.7	1.69×10^{08}	0.4	4.57×10^{09}	0.6
31	C═C−C−C(C_2)−C−C•	3.37×10^{07}	0.85	4.1	−16.6	1.06×10^{08}	0.6	4.31×10^{09}	0.7
32	C═C−C(C_2)−C−C−C•	1.18×10^{07}	0.99	4.3	−17.4	6.85×10^{07}	0.9	3.72×10^{09}	0.8
33	C_2−C═C−C−C−C−C•	2.01×10^{07}	0.90	4.3	−16.6	7.25×10^{07}	0.8	3.42×10^{09}	0.8
	1,7-exo-cycloaddition	**2.79×10^{04}**	**1.40**	**4.2**	**−21.9**	**2.45×10^{06}**		**1.93×10^{08}**	
34	C═C−C−C−C−C−C•	1.53×10^{05}	1.26	5.1	−22.6	2.39×10^{06}	1.0	2.89×10^{08}	0.7
35	C═C−C−C−C−C−C•−C	1.87×10^{04}	1.43	4.1	−21.3	2.21×10^{06}	1.1	1.62×10^{08}	1.2
36	C═C−C−C−C−C−C_3•	2.02×10^{03}	1.67	2.6	−20.1	4.62×10^{06}	0.5	1.69×10^{08}	1.1
37	trans-C−C═C−C−C−C−C-C•	4.14×10^{05}	1.14	5.0	−22.5	3.19×10^{06}	0.8	3.21×10^{08}	0.6
38	cis-C-C═C−C−C−C−C-C•	4.27×10^{05}	1.06	5.0	−23.5	2.04×10^{06}	1.2	1.81×10^{08}	1.1
39	C═C_2−C−C−C−C−C• *	2.46×10^{04}	1.32	6.1	−20.2	1.99×10^{05}		5.09×10^{07}	
40	C_2−C═C−C−C−C−C−C•	2.16×10^{05}	1.18	4.3	−23.1	4.40×10^{06}	0.6	2.80×10^{08}	0.7

[a]The units for A and k_{TST}, k_{rule} are s^{-1}, and are kcal/mol for E. [b]The k(rate rule) term has been calculated using the bold rate rule listed for each subset; the single star * means the reactions are excluded during the rate rule development. [c]The notation for others are the same as Table 1.

sum of the rate constants, although the latter one is generally favored.

Similar to the H atom shift reactions, both the endo- and exo-cycloaddition rate constants also group according to the size of the ring formed in the transition state/product. A comparison of the rate constants for the simplest *n*-alkenyl radicals in each one of these categories is shown in Figure 5. In both cases, the pre-exponential factors decrease as the ring size expands. For the endo-cycloadditions (solid lines), the activation energies also decrease with the ring expansion. For the exo-cycloadditions (dashed lines), the activation energy is predicted to be surprisingly low to form the three-member ring. It increases in going to a four-member ring, and then decreases sequentially when forming larger rings. The low barrier for the formation of the three-membered ring has previously been reported.[35] While this is unusual, it is not unprecedented. The barriers for the formation of dioxiranylmethyl radical from peroxy vinyl radical,[47] and oxirane + OH from β-hydroperoxy alkyl radicals[41,48] are also lower than expected. The trends observed in this study will be discussed in more detail later in the text.

Within each one of the ring-size categories, we have examined the impact of substitution along the carbon backbone. The results suggest that the pre-exponential factors

DOI: 10.1021/jp511017z
J. Phys. Chem. A XXXX, XXX, XXX−XXX

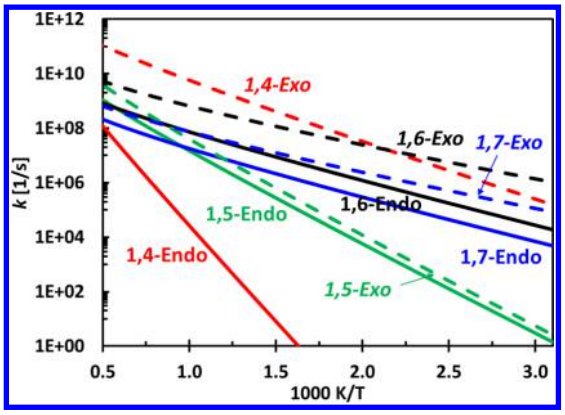

Figure 5. Comparison of rate constants for the simplest endo- (solid lines) and exo- (dashed lines) cycloaddition reactions for unsubstituted *n*-alkenyl radicals.

are insensitive to the presence of a substituent(s), and within a given category they all group closely together (within a factor of ~2). In general, substitution tends to decrease the reaction barrier. This is illustrated in Figure 6, which compares the rate constants for the 1,5-cycloaddition reactions. The comparisons for other cycloaddition reactions are provided in Supporting Information, Figures S3 and S4. For the endo-reactions, there is a decrease in the barrier by less than 1 kcal/mol with the addition of one methyl group and a further decrease with the addition of a second methyl group by ~1 kcal/mol. The barriers for reactions where the double bond is located in the interior of the carbon chain (i.e., the alkenyl radical contains substituents on the 1-position of the double bond) depend upon whether the reactant is in the cis- or trans-configuration. For the singly substituted trans-alkenyl radicals, the general trend is followed, and a decrease in the barrier is observed. However, if the substituted alkenyl radical is in the cis-form, the barrier increases. Roughly the same magnitude of increase (0.5 to 1.5 kcal/mol) is observed for the addition of two methyl groups on the 1-position, as seen in Figure 6a. This increase is attributed to unfavorable sterics of the axially positioned methyl group on the carbon where addition occurs in the transition state structure. Since the radical adds perpendicularly to the double bond, the geometry of the substituted 1-carbon is essentially locked-in, and the ring cannot flex to relieve the unfavorable interaction. If, however, there is an axially positioned methyl group on other carbon atoms, the ring can adjust to minimize the unfavorable interaction. Similar, but slightly more dramatic, trends are observed for the exo-cycloaddition reactions. In this case, the addition of one methyl lowers the barrier by as much as 2 kcal/mol, and two methyl groups can lower it by up to 3.5 kcal/mol. Here the outlier reaction involves substitution of a methyl group on the 2-position of the double bond resulting in an increase in the barrier by roughly 0.5 to 1.5 kcal/mol (see Figure 6b). This results in the same unfavorable interaction as in the outlier endo-cases.

The pre-exponential factors for the exo-pathway are higher than those for the competing endo-pathway due to fewer hindered rotors that are lost in the smaller sized ring. The contribution from the higher pre-exponential factors would, however, typically be offset by the higher barrier associated with the formation of the smaller ring. Inspection of the two sets of rate constants in Figure 5 shows that this is clearly not the case. The exo-cycloaddition pathways are favored over the endo-pathways, even for cases where the formation of the endo-products are favored thermodynamically. Possible reasons for this will be discussed in the next section. However, there are a few select cases where the endo-pathway is favored over the exo-pathway. These involve alkenyl radicals that have a substituent on the 2-position, which significantly lowers the rate of addition of the exo-pathway. For example, cycloaddition of the 3-methyl-1-hex-5-enyl radical (C=C(C)CCCC•) predominantly proceeds via the endo-pathway at lower temperatures (shown by the blue solid and dashed lines in Figure 7). Several previous studies[49−53] have leveraged the reactivity of substituted alkenyl radicals to alter the reaction selectivity.

For both the endo- and exo-cycloaddition reactions, a series of rate rules were developed based upon the size of ring formed in the transition state structure/product. Even though the results clearly show that substitution alters the reaction barrier as well as the heat of reaction, there was no consistent variation of barrier height with the enthalpy change. Thus, only one rate rule was developed for each one of these subcategories. In general, the rule can predict the individual rate constants to within a factor of 3 at 500 and 1500 K. The exceptions to this are the outlier cases discussed above, which were not used in the derivation of the rate rule. In these cases, the rate rule

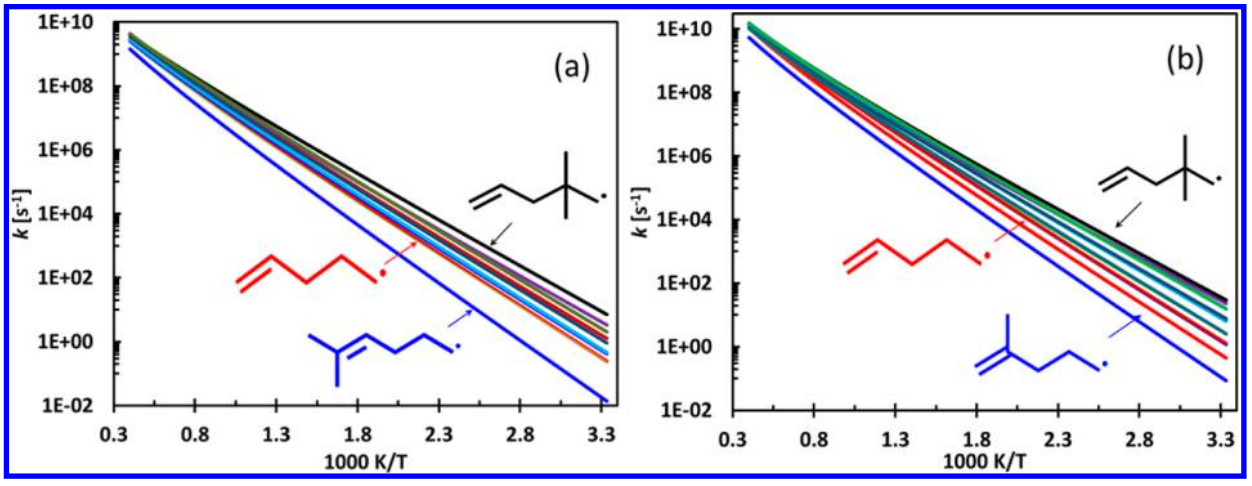

Figure 6. Rate constants for the (a) 1,5-endo-cycloaddition and (b) 1,5-exo-cycloaddition with and without substituted groups.

DOI: 10.1021/jp511017z
J. Phys. Chem. A XXXX, XXX, XXX−XXX

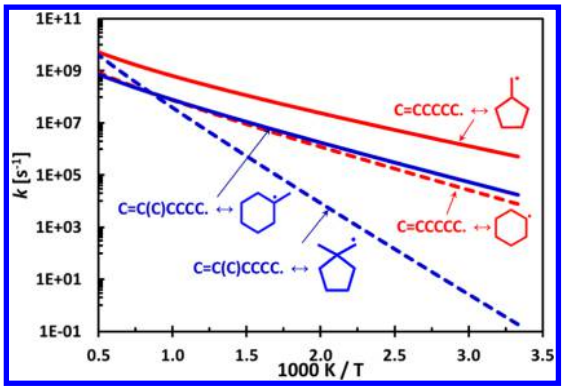

Figure 7. Comparison of the rate constant for the 1,6-exo- and endo-cycloaddition reactions for 5-hex-1-enyl and 5-methyl-5-hex-1-enyl radicals.

overpredicts the rate constants by roughly an order of magnitude. Other outlier cases involve select reactions in the 1,4- and 1,5-exo-reactions, which are within a factor of 5 of the rule. Since the 1,4-exo-cycloadditions are fast, one may need to exercise caution when employing this particular rule. The wider deviation in the agreement with the rate rule, as opposed to the better agreement in the H atom shift reactions, is due to the sensitivity of the barrier with respect to substitution. The impact of this is greatest for the reactions that form smaller sized rings.

There have been a number of prior studies that have focused on the endo-cycloaddition reactions. In Figure 8 we compare the rate constants for the endo-cycloaddition of the 1-pent-4-enyl and 1-hex-5-enyl radicals (C═CCCC• and C═CCCCC•) to other experimental and theoretical values in the literature. The experimental data for the pentenyl cycloaddition reaction is from the shock tube studies of Awan et al.[22] Gierczak et al.[54] also studied this reaction using a chemical activation approach. Both experiments used RRKM calculations to obtain rate parameters for the various competing reactions. The agreement between the rate constants obtained in this work, those from the other two computational studies, and the experimental data is quite reasonable. The recommendation by Tsang[55] is significantly lower. Good agreement is also obtained for the reverse ring opening reaction; this comparison is provided in the Supporting Information in Figure S5. The experimental data for the 1-hex-5-enyl radical is from the kinetic studies of oxidation of cyclopentane by Handford-Styring and Walker.[56] The value reported here is in good agreement with this data. However, the calculated rate constants of Matheu et al.[26] and Sirjean et al.[33] are much higher. The pre-exponential factor calculated by Sirjean et al.[5] is within a factor of 2 of their value for the 1-pen-4-entyl closure. One would expect a larger difference in the two, given that there is an additional hindered rotor lost in the transition state.

Very few rate constants are available in the literature for the exo-cycloaddition of alkenyl radicals. Chatgilialoglu et al.[57] measured the rate constants for the 1,6-cycloaddition of 1-hex-5-enyl radical (C═CCCCC•) to form cyclopentyl-carbinyl radical using kinetic EPR spectroscopy and laser flash photolysis. Wu et al.[58] calculated the rate constant at 298 K using the UB3LYP functional. Sirjean et al.[33] calculated the rate constant for this reaction over the temperature range 500–2000 K. Figure 9 compares these results with this work. The values determined in this work agree with those in Chatgilialoglu et al.[57] and Wu et al.[58] It also agrees with Sijean et al.[33] at the lower temperatures, but deviates significantly at higher temperatures. Wang et al.[35] calculated the rate constant for several secondary alkenyl radicals for the 1,4- to 1,6-exo-cycloaddition. The comparison with those calculated in this study are provided in the Supporting Information, Figure S6. Generally, the energy barriers obtained in this study are consistent with those by Wang et al.,[35] but the pre-exponential factors are higher by about 1 order of magnitude.

DISCUSSION

Bimolecular and Ring Strain Components of the Activation Energies. According to the Benson model,[1] the activation energy for the alkyl radical H atom shift and alkenyl radical cycloaddition reactions can be considered to consist of two components: a contribution from a bimolecular H atom abstraction or addition reaction, respectively, plus the ring strain ($E_a = E_{bi} + E_{strain}$). For both reaction types, the contribution from the respective bimolecular reaction is the same for the various ring-size categories, so the changes in the activation energies with increasing ring size is simply due to changes in the ring strain.

Table 4 summarizes the rate rules for the alkyl radical H atom shift reactions. In order to better observe the trends in the

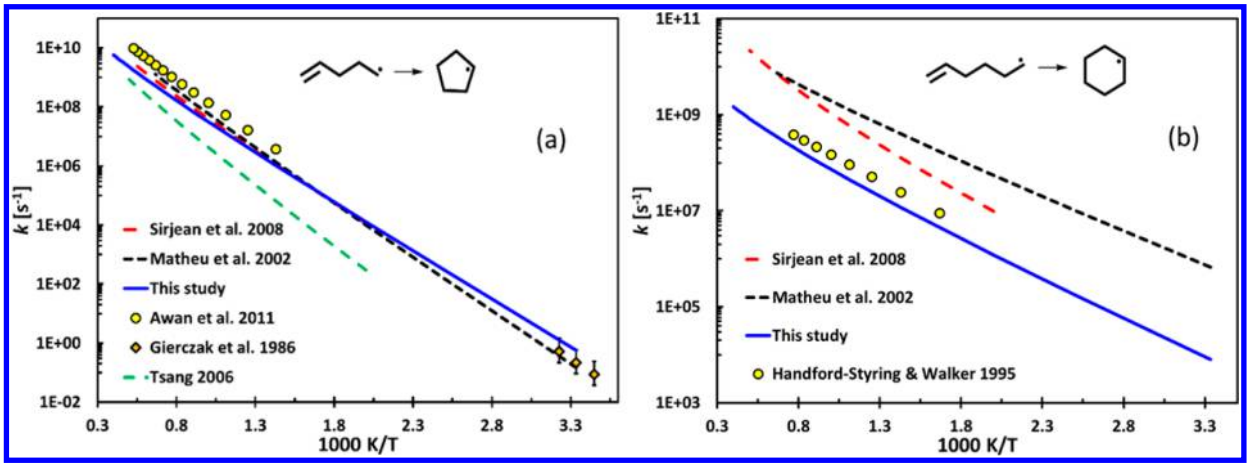

Figure 8. Comparison of the rate constant for endo-cycloaddition reactions (a) $C_5H_9 \rightarrow$ c-C_5H_9 and (b) $C_6H_{11} \rightarrow$ c-C_6H_{11} obtained in this study and those reported in the literature.

DOI: 10.1021/jp511017z
J. Phys. Chem. A XXXX, XXX, XXX–XXX

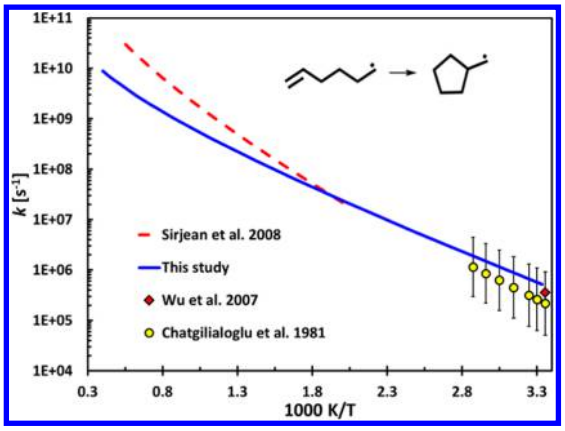

Figure 9. Comparison of the rate constant for exo-cycloaddition reactions C═CCCCC• → cyclopentyl-carbinyl radical in this study and in the literature.

rate parameters with increasing ring size, we provide the rate rules in simple Arrhenius form at 298 K and over a temperature range of 500 to 1500 K. The values at 298 K are provided because they help facilitate the construction of potential energy surfaces (PES), since the thermodynamic properties for the stable species are easily obtained at this temperature using group additivity. On the other hand, the parameters at 500−1500 K are more relevant for typical pyrolysis and combustion conditions. (It is important to keep in mind that these reactions display significant non-Arrhenius behavior, and the modified Arrhenius form is preferred for kinetic modeling studies.) The corresponding rate parameters for the bimolecular H atom abstraction reactions are provided in Table 5. Note that the bimolecular abstraction reactions are divided into the same six subcategories (pp, ss, tt, ps, st, and tt) as the H atom shift reactions are. (A representative comparison of the calculated abstraction rate constants to experiments is given in the Supporting Information Figure S7). The ring strain values included in Table 4 are obtained by subtracting the corresponding bimolecular activation energy in Table 5 from the overall activation energy (either at 298 K or over the 500−1500 K range). A similar procedure is used to obtain ring strain estimates for the cycloaddition reactions. The rate parameters for the endo- and exo-cycloaddition reactions are summarized in Tables 6 and 7; the corresponding data for the bimolecular addition reactions are listed in Table 8. For the cycloaddition and the bimolecular addition reactions, the degree of branching around the double bond and the radical site in the reactant(s) is similar. The ring strain energies are obtained for each reaction in Tables 2 and 3 (by pairing each unimolecular reaction with its corresponding bimolecular reaction), and the average value for each ring-size category is reported in Tables 6 and 7, respectively. In all cases, the ring strain slightly decreases as the temperature increases. This is because the bimolecular reactions display a stronger temperature dependence than the unimolecular reactions do.

Figure 3 compares the Evans−Polanyi relationships for the H atom shift reactions to that of the bimolecular abstraction reactions. The slopes for the various reaction categories are similar, and the difference in the *y*-axis between a given H atom shift reaction and its corresponding abstraction reaction is the ring strain. Consistent with expectations, the three- and four-member ring transition states have the highest ring strain followed by the five-member ring transition state. However, an interesting observation is that the ring strain (hence the activation energy) for six-member ring is slightly higher than that of the seven-member ring transition state; the ring strain increases for the eight-member ring structure. This result is consistent with previous studies in the literature, but it is in contrast with the ring strain energies of cycloalkanes,[59] which increase in going from cyclohexane, where there is no strain, to cycloheptane (see Table 9). Tsang and co-workers[2] investigated the thermal decomposition of *n*-heptyl and *n*-octyl radicals in a shock tube environment. These results suggest that the activation energy for the 1,6-H shift (seven-member ring) is either equivalent or less than the 1,5-H shift (six-member ring). The theoretical study by Davis and Francisco[4] also indicated slightly lower barrier height for 1,6-H shift; this is attributed to the C−H−C bond angle formed from the three reacting atoms in 1,6-H shift isomerization, which actually resembles cyclohexane instead of cycloheptane.

The ring strain energies for the endo-cycloadditions are comparable to those of the corresponding H atom shift transition states. In this case, however, the ring strain for the six-member ring is slightly lower than that for the seven-member ring, although the difference between the two is still much lower than the difference between cyclohexane and cycloheptane (Table 9). The ring strain energies for the exo-cycloadditions are quite unexpected. Most notable is that the ring strain for the three-member ring is less than that for the four-member ring, and both of these are unusually low. There is essentially no strain for the five- and six-member rings.

Relationship between Hindered Rotors and Pre-exponential Factors. Examination of the pre-exponential factors shows that they systematically decrease with increasing ring size. Figure 10 presents the correlation between the "normalized" pre-exponential factors (i.e., on a per H basis) to the number of rotors lost in the transition states for the alkyl radical H-shift reactions (in blue). The pre-exponential factors drop by almost a factor of 10 as the transition state ring increases by one more carbon atom (i.e., another hindered rotor lost in the transition state). The intercept is comparable to the TST pre-exponential factor (ek_b/h·1000 K). Hayes and Burgess[3] observed a similar decrease in the pre-exponential factors for three- to six-member ring when they examined a narrow temperature range of 1000−1300 K. Sirjean et al.[5] examined the contribution of loss of hindered rotors to the activation entropy for 1,4- to 1,7-H shift reactions involving heptyl and octyl radicals. The per rotor entropy loss was found to be constant.

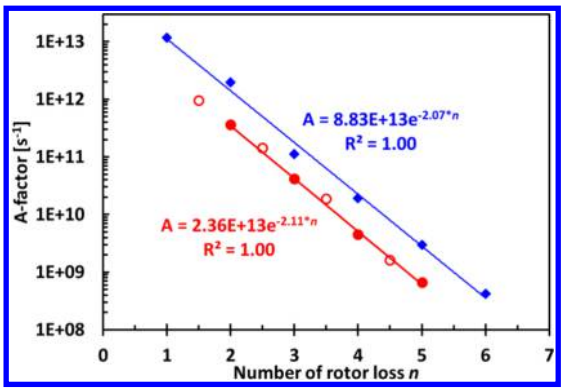

Figure 10. Correlation between the pre-exponential factor and loss of hindered rotors (blue dots and line: H-shift; filled red dots and line: endo-cycloaddition; open red dots: exo-cycloaddition) at 500−1500 K.

DOI: 10.1021/jp511017z
J. Phys. Chem. A XXXX, XXX, XXX−XXX

Table 4. Summary of Rate Rules, Ring Strains at 298 K and 500−1500 K, and Reaction Enthalpy Changes for H-Shift Isomerization Reactions[a,b]

					298 K			500−1500 K			
		modified Arrhenius parameters			Arrhenius parameters			Arrhenius parameters			
#	reaction type	A_H	n	E	A'_H	E_a	E_{strain}	A''_H	E_a'	E'_{strain}	$\Delta_R H^{298}$ [kcal/mol]
	1,2-H shift										
1	**pp**	**4.71 × 10^06**	**1.81**	**37.1**	8.77 × 10^11	38.2	24.1	7.69 × 10^12	40.5	23.0	0.0
2	**ss rate rule**	**4.02 × 10^06**	**1.86**	**36.6**	1.06 × 10^12	37.7	25.4	9.95 × 10^12	40.1	24.1	−0.1
3	**tt**	**8.38 × 10^07**	**1.60**	**38.1**	3.77 × 10^12	39.1	29.8	2.58 × 10^13	41.1	27.9	0.0
4	**st rate rule**	**5.74 × 10^07**	**1.53**	**35.7**	1.58 × 10^12	36.6	26.6	9.70 × 10^12	38.5	25.0	−2.1
5	**ps rate rule**	**3.24 × 10^07**	**1.57**	**35.3**	1.23 × 10^12	36.3	24.5	8.56 × 10^12	38.4	23.2	−2.8
6	**pt rate rule**	**1.51 × 10^08**	**1.39**	**33.0**	1.70 × 10^12	33.8	24.2	9.38 × 10^12	35.7	23.0	−5.1
						average	25.8			24.4	
						STDEV	2.2			1.9	
	1,3-H shift										
1	**pp rate rule**	**5.90 × 10^04**	**2.17**	**35.4**	1.20 × 10^11	36.7	22.6	1.48 × 10^12	39.3	21.8	0.0
2	**ss rate rule**	**1.11 × 10^05**	**2.16**	**35.1**	2.12 × 10^11	36.4	24.1	2.62 × 10^12	38.9	22.9	−0.1
3	**tt**	**2.54 × 10^05**	**2.03**	**33.6**	2.09 × 10^11	34.8	25.5	2.26 × 10^12	37.3	24.1	0.0
4	**st**	**7.12 × 10^05**	**1.82**	**33.6**	1.44 × 10^11	34.7	24.7	1.19 × 10^12	36.8	23.3	−1.6
5	**ps rate rule**	**5.32 × 10^05**	**1.93**	**33.8**	2.24 × 10^11	34.9	23.1	2.09 × 10^12	37.2	22.1	−2.9
6	**pt**	**1.73 × 10^06**	**1.79**	**32.5**	2.69 × 10^11	33.6	24.0	2.12 × 10^12	35.7	23.0	−4.4
						average	24.0			22.8	
						STDEV	1.0			0.8	
	1,4-H shift										
1	**pp rate rule**	**7.59 × 10^04**	**1.74**	**19.8**	8.49 × 10^09	20.8	6.7	5.61 × 10^10	22.6	5.1	−0.4
2	**ss rate rule**	**3.87 × 10^05**	**1.66**	**19.1**	2.65 × 10^10	20.1	7.8	1.64 × 10^11	21.9	5.9	−0.1
3	**tt**	**7.48 × 10^04**	**1.81**	**16.8**	1.37 × 10^10	17.8	8.5	1.02 × 10^11	19.8	6.6	0.0
4	**st**	**5.02 × 10^05**	**1.52**	**17.2**	1.34 × 10^10	18.1	8.1	7.07 × 10^10	19.7	6.2	−1.8
5	**ps rate rule**	**3.77 × 10^05**	**1.63**	**17.9**	2.05 × 10^10	18.9	7.1	1.20 × 10^11	20.6	5.4	−2.9
6	**pt**	**3.35 × 10^06**	**1.39**	**16.5**	3.58 × 10^10	17.3	7.7	1.58 × 10^11	18.7	6.0	−4.6
						average	7.6			5.9	
						STDEV	0.7			0.5	
	1,5-H shift										
1	**pp rate rule**	**4.59 × 10^04**	**1.68**	**12.6**	3.56 × 10^09	13.6	−0.5	2.08 × 10^10	15.3	−2.2	−0.2
2	**ss rate rule**	**6.37 × 10^04**	**1.64**	**12.0**	3.78 × 10^09	13.0	0.7	2.13 × 10^10	14.6	−1.4	−0.1
3	**tt**	**1.69 × 10^04**	**1.73**	**9.6**	1.84 × 10^09	10.6	1.3	1.17 × 10^10	12.4	−0.8	0.0
4	**st**	**1.53 × 10^05**	**1.40**	**10.5**	1.78 × 10^09	11.3	1.3	7.57 × 10^09	12.6	−0.9	−1.6
5	**ps rate rule**	**1.31 × 10^05**	**1.62**	**11.1**	6.62 × 10^09	12.0	0.2	3.57 × 10^10	13.6	−1.5	−3.0
6	**pt**	**1.03 × 10^06**	**1.27**	**9.4**	5.23 × 10^09	10.2	0.5	1.91 × 10^10	11.4	−1.3	−4.7
						average	0.6			−1.4	
						STDEV	0.7			0.5	
	1,6-H shift										
1	**pp rate rule**	**2.46 × 10^03**	**1.79**	**11.9**	3.98 × 10^08	13.0	−1.1	2.49 × 10^09	14.7	−2.8	−0.3
2	**ss**	**6.71 × 10^03**	**1.75**	**10.7**	8.27 × 10^08	11.8	−0.5	3.93 × 10^09	14.0	−2.0	0.0
3	**tt**	**1.54 × 10^03**	**1.78**	**8.2**	2.29 × 10^08	9.2	−0.1	1.45 × 10^09	11.0	−2.2	0.0
4	**st**	**1.65 × 10^04**	**1.50**	**9.0**	3.90 × 10^08	9.9	−0.1	1.78 × 10^09	11.3	−2.2	−1.6
5	**ps rate rule**	**1.29 × 10^04**	**1.67**	**10.2**	9.40 × 10^08	11.2	−0.6	5.21 × 10^09	12.8	−2.3	−2.9
6	**pt**	**5.15 × 10^04**	**1.35**	**8.6**	4.26 × 10^08	9.4	−0.2	3.19 × 10^09	10.6	−2.1	−4.5
						average	−0.4			−2.3	
						STDEV	0.4			0.3	
	1,7-H shift										
1	**pp**	**4.28 × 10^01**	**2.10**	**15.1**	5.48 × 10^07	16.3	2.2	5.21 × 10^08	18.5	1.0	0.0
2	**ss**	**9.92 × 10^01**	**2.00**	**13.2**	6.50 × 10^07	14.4	2.1	5.04 × 10^08	16.3	0.3	0.0
3	**st**	**1.93 × 10^02**	**1.74**	**11.0**	2.16 × 10^07	12.0	2.0	1.24 × 10^08	13.6	0.1	−1.7
4	**ps**	**5.31 × 10^02**	**1.81**	**13.2**	9.66 × 10^07	14.3	2.5	5.91 × 10^08	15.9	0.8	−2.9
5	**pt**	**1.55 × 10^03**	**1.61**	**10.7**	7.37 × 10^07	11.6	2.0	3.56 × 10^08	13.0	0.3	−4.5
						average	2.2			0.5	
						STDEV	0.2			0.4	

[a]The units for A_H, A'_H, and A''_H are s^{-1}, and are kcal/mol for E, E_a, E_a', E_{strain}, and E_{strain}'. [b]The notation for others are the same as Table 1.

DOI: 10.1021/jp511017z
J. Phys. Chem. A XXXX, XXX, XXX−XXX

Table 5. Calculated Rate Parameters for Representative Hydrogen Abstraction[a,b]

H-abstraction reactions	n_H	300−2500 K A_H	n	E	298 K A'_H	E_a	500−1500 K A''_H	E_a'	$\Delta_R H^{298}$ [kcal/mol]
pp									
$C_2H_5 + C_2H_6 \leftrightarrow C_2H_5 + C_2H_6$	6	2.07×10^{01}	3.16	12.2	3.25×10^{10}	14.0	2.12×10^{12}	17.5	0.0
$CCC^{\bullet} + CCC \leftrightarrow CCC + CCC^{\bullet}$	3	2.68×10^{01}	3.21	12.1	5.96×10^{10}	14.0	2.02×10^{12}	17.5	0.0
$C_2H_5 + CCC \leftrightarrow C_2H_6 + CCC^{\bullet}$	6	2.63×10^{01}	3.18	12.3	4.74×10^{10}	14.2	1.58×10^{12}	17.7	0.3
$C_2H_5 + CCCC \leftrightarrow C_2H_6 + CCCC^{\bullet}$	6	3.82×10^{01}	3.17	12.2	6.25×10^{10}	14.1	2.07×10^{12}	17.6	0.1
$C_2H_5 + CC(C)C \leftrightarrow C_2H_6 + CC(C)C^{\bullet}$	9	2.62×10^{01}	3.18	12.2	4.72×10^{10}	14.0	1.59×10^{12}	17.5	0.7
					average	14.1		17.5	
ss					STDEV	0.1		0.1	
$CC^{\bullet}C + CCC \leftrightarrow CCC + CC^{\bullet}C$	2	2.68×10^{00}	3.32	10.5	1.17×10^{10}	12.5	4.71×10^{11}	16.2	0.0
$CC^{\bullet}C + CCCC \leftrightarrow CCC + CCC^{\bullet}C$	4	2.98×10^{00}	3.30	10.3	1.14×10^{10}	12.3	4.43×10^{11}	15.9	0.2
$CCC^{\bullet}C + CCC \leftrightarrow CCCC + CC^{\bullet}C$	2	3.98×10^{00}	3.34	10.1	2.08×10^{10}	12.1	4.25×10^{11}	15.8	−0.2
					average	12.3		16.0	
tt					STDEV	0.2		0.2	
$CC(C)^{\bullet}C + CC(C)C \leftrightarrow CC(C)C + CC(C)^{\bullet}C$	1	3.78×10^{-02}	3.45	7.1	4.15×10^{08}	9.1	1.96×10^{10}	13.0	0.0
$CC(C)^{\bullet}C + CC(C)CC \leftrightarrow CC(C)C + CC(C)^{\bullet}CC$	1	5.99×10^{-02}	3.46	7.4	7.07×10^{08}	9.5	3.41×10^{10}	13.4	−0.6
					average	9.3		13.2	
st					STDEV	0.3		0.3	
$CC^{\bullet}C + CC(C)C \leftrightarrow CCC + CC(C)^{\bullet}C$	1	4.79×10^{00}	3.13	8.2	6.20×10^{09}	10.0	2.00×10^{11}	13.5	−1.5
$CCC^{\bullet}C + CC(C)C \leftrightarrow CCCC + CC(C)^{\bullet}C$	1	2.31×10^{00}	3.18	8.1	4.07×10^{09}	10.0	1.38×10^{11}	13.5	−1.7
					average	10.0		13.5	
ps					STDEV	0.1		0.0	
$C_2H_5 + CCC \leftrightarrow C_2H_6 + CC^{\bullet}C$	2	1.42×10^{02}	3.05	10.1	1.02×10^{11}	11.9	2.92×10^{12}	15.2	−2.8
$C_2H_5 + CCC \leftrightarrow C_2H_6 + CC^{\bullet}CC$	4	1.54×10^{02}	3.05	10.0	1.14×10^{11}	11.8	3.28×10^{12}	15.1	−2.7
$CCC^{\bullet} + CCC \leftrightarrow CCC + CC^{\bullet}C$	2	1.14×10^{02}	3.12	10.0	1.33×10^{11}	11.8	4.12×10^{12}	15.2	−3.2
					average	11.8		15.2	
pt					STDEV	0.1		0.1	
$C_2H_5 + CC(C)C \leftrightarrow C_2H_6 + CC(C)^{\bullet}C$	1	1.04×10^{03}	2.93	8.0	3.46×10^{11}	9.7	8.66×10^{12}	12.9	−4.4
$C_2H_5 + CC(C)CC \leftrightarrow C_2H_6 + CC(C)^{\bullet}CC$	1	1.23×10^{03}	2.86	7.7	2.60×10^{11}	9.4	6.02×10^{12}	12.5	−4.4
					average	9.6		12.7	
					STDEV	0.2		0.3	

[a]The units for A_H, A'_H, and A''_H are $cm^3/(mol \cdot s)$, and are kcal/mol for E, E_a, and E_a'. [b]The notation for others are the same as Table 1.

Table 6. Summary of Rate Rules and Ring Strain Energies for the Endo-cycloaddition Reactions[a]

reactions	modified Arrhenius parameters A	n	E	298 K Arrhenius parameters A'	E_a	E_{strain}	500−1500 K Arrhenius parameters A''	E_a'	E_{strain}'	$\Delta_R H^{298}$ [kcal/mol]
1,4-endo-cycloaddition	**6.34×10^{07}**	**1.12**	**29.5**	1.12×10^{11}	30.1	24.4 ± 1.0	3.62×10^{11}	31.4	22.5 ± 1.1	3.9
1,5-endo-cycloaddition	**9.87×10^{06}**	**1.06**	**13.0**	1.21×10^{10}	13.6	8.1 ± 0.6	4.18×10^{10}	14.6	6.0 ± 0.7	−18.7
1,6-endo-cycloaddition	**2.79×10^{06}**	**0.96**	**6.0**	1.78×10^{09}	6.6	0.6 ± 0.7	4.49×10^{09}	7.4	−1.4 ± 0.7	−22.5
1,7-endo-cycloaddition	**3.98×10^{04}**	**1.27**	**6.2**	2.01×10^{08}	7.0	1.1 ± 0.6	6.69×10^{08}	8.2	−0.6 + 0.5	−19.1

[a]The units for A, A', and A'' are s^{-1}, and are kcal/mol for E, E_a, E_a', E_{strain}, and E_{strain}'.

Table 7. Summary of the Rate Rules and Ring Strain Energies for the Exo-cycloaddition Reactions[a]

reactions	modified Arrhenius parameters A	n	E	298 K Arrhenius parameters A'	E_a	E_{strain}	500−1500 K Arrhenius parameters A''	E_a'	E_{strain}'	$\Delta_R H^{298}$ [kcal/mol]
1,4-exo-cycloaddition	**1.08×10^{07}**	**1.45**	**6.6**	1.80×10^{11}	7.5	2.2 ± 1.0	9.61×10^{11}	9.2	−0.1 ± 1.2	2.4
1,5-exo-cycloaddition	**1.35×10^{06}**	**1.48**	**12.2**	2.75×10^{10}	13.0	6.7 ± 0.8	1.45×10^{11}	14.7	5.0 ± 0.9	1.5
1,6-exo-cycloaddition	**1.60×10^{06}**	**1.20**	**3.8**	4.96×10^{09}	4.5	−2.2 ± 0.7	1.87×10^{10}	5.8	−4.1 ± 0.6	−16.4
1,7-exo-cycloaddition	**2.79×10^{04}**	**1.40**	**4.2**	3.35×10^{08}	5.0	−1.8 ± 0.3	1.62×10^{09}	6.6	−3.5 ± 0.5	−21.9

[a]The units for A, A', and A'' are s^{-1}, and are kcal/mol for E, E_a, E_a', E_{strain}, and E_{strain}'.

DOI: 10.1021/jp511017z
J. Phys. Chem. A XXXX, XXX, XXX−XXX

Table 8. Calculated Rate Parameters for Representative Addition Reactions to Olefins by Alkyl Radicals[a,b,c]

reactions	300−2500 K			298 K		500−1500 K		$\Delta_R H^{298}$ [kcal/mol]	serve as bimolecular reactions
	A	n	E	A'	E_a	A''	E_a'		
C_2H_5 + C=CC ↔ CCCC•C	4.37×10^{03}	2.47	5.04	6.50×10^{10}	6.50	9.59×10^{11}	9.15	−22.3	T2:1, 6, 8, 12, 17−18, 20−21, 23, 28−29, 30, 32−34, 36
C_2H_5 + C=CC ↔ CCCC$_2$•	1.37×10^{03}	2.61	6.27	5.17×10^{10}	7.81	9.10×10^{11}	10.6	−20.6	T3:1, 6, 8, 10, 15, 16, 18, 19, 21, 27−32, 34
CC•C + C=CC ↔ CC$_2$CC•C	5.26×10^{02}	2.70	4.34	3.65×10^{10}	5.93	3.59×10^{11}	8.89	−21.2	T2:2, 13, 24, 37
CC•C + C=CC ↔ CC$_2$CC$_2$•	5.08×10^{01}	2.98	5.11	2.30×10^{10}	6.88	3.19×10^{11}	10.2	−18.8	T3:2, 11, 22, 35
C_3C• + C=CC ↔ C_3CC•C	2.83×10^{01}	3.03	2.41	1.89×10^{10}	4.21	5.55×10^{11}	7.59	−21.0	T2:3, 14, 25, 38
C_3C• + C=CC ↔ C_3CC_2•	9.24×10^{00}	3.30	3.95	3.66×10^{10}	5.90	5.00×10^{11}	9.64	−22.4	T3:3, 12, 23, 36
C_2H_5 + cis-CC=CC ↔ CCCC$_2$•	2.90×10^{03}	2.58	5.60	9.07×10^{10}	7.12	1.53×10^{12}	9.92	−22.2	T2:5, 15, 26, 39, and T3:4, 14, 25, 38
C_2H_5 + trans-CC=CC ↔ CCCC$_2$•	3.40×10^{03}	2.49	5.64	5.73×10^{10}	7.11	1.73×10^{12}	9.79	−21.1	T2:4, 16, 27, 40, and T3:5, 13, 24, 37
C_2H_5 + CC=CC$_2$ ↔ CCC(C$_2$)C•C	1.21×10^{02}	2.76	6.11	1.32×10^{10}	7.74	9.57×10^{11}	9.15	−20.7	T2:11, 22, 35, 42
C_2H_5 + CC=CC$_2$ ↔ CCC$_2$C•C$_2$	3.61×10^{03}	2.49	4.99	6.31×10^{10}	6.47	9.57×10^{11}	9.15	−22.2	T3:9, 20, 33, 40
C_2H_5 + C_2C=C ↔ CCCC•C$_2$	1.46×10^{04}	2.38	4.95	1.24×10^{11}	6.36	1.65×10^{12}	8.90	−21.9	T2:7, 19, 31, 41
C_2H_5 + C_2C=C ↔ CCCC$_3$•	1.07×10^{02}	2.83	6.99	1.81×10^{10}	8.67	4.17×10^{11}	11.8	−19.2	T3:7, 17, 26, 39

[a]The units for A, A', and A'' are cm^3/(mol·s), and are kcal/mol for E, E_a, and E_a'. [b]Notations are the same as in Table 1. [c]T2 and T3 are Tables 2 and 3.

Table 9. Ring Strain Energy of H-Shift Isomerization, Endo-cycloaddition, Exo-cycloaddition, and Cycloalkanes[59] at 298 K

ring size	ring strain energy at 298 K (kcal/mol)			
	H-shift	endo-cycloaddition	exo-cycloaddition	cycloalkanes[59]
3	25.8 ± 2.2		2.2 ± 1.0	27.7
4	24.0 ± 1.0	24.4 ± 1.0	6.7 ± 0.8	26.8
5	7.6 ± 0.7	8.1 ± 0.6	−2.2 ± 0.7	7.1
6	0.6 ± 0.7	0.6 ± 0.7	−1.8 ± 0.3	0.7
7	−0.4 ± 0.4	1.1 ± 0.6		6.8
8	2.2 ± 0.2			10.3

The pre-exponential factors for the endo- and exo-cycloaddition reactions are also shown in Figure 10. For the exo-cycloaddition reactions (open red symbols), the C−C=C bending vibration is not constrained in the transition state; this leads to an increased entropy (compared to the endo-transition state). To account for this, we assume a gain of 0.5 rotor; this allows the data for the exo-reactions to fall on the trend line for the endo-data. Similar to the H atom shift reactions, the pre-exponential factors drop by almost a factor of 10 as the transition state ring is expanded. For a given rotor loss, the pre-exponential factors for the endo-cycloadditions are ∼4 times smaller than those for the respective H atom shift reactions. In this temperature range, the smaller pre-exponential factors are not due to the difference in tunneling correction factors. At 1000 K, the tunneling correction factor for the cycloaddition reactions is ∼1.1, while that for the H-shift reactions is only slightly higher at ∼1.5. Thus, while the ring strains are comparable, more entropy is lost in the cycloaddition transition states than in the H-shift transition states. The primary difference between the two transition states is that there is a CH_2 group in the ring for the endo-cycloadditions versus an H atom in the H-shift reactions.

In summary, the rate parameters for both the H atom shift and cycloaddition reactions can be estimated surprisingly well using a Benson-type model, allowing for a simple check on the plausibility of proposed rate constants for these type reactions. In the past, without the benefit of electronic structure calculations and very limited data, the ring strain component of the activation energy was often assumed to be similar to that of cycloalkanes. This work confirms that, for some cases, this is not a good assumption. While these values can be easily estimated using the Benson model, the series of rate rules that are provided in modified Arrhenius form provide more accurate estimates of these values.

Examination of the Cycloaddition Reaction Branching Ratio. The above analysis shows that the exo-cycloaddition reactions are generally favored over the endo-reactions. Not only are the pre-exponential factors higher, due to loss of one less hindered rotor in the transition state structure, but the activation energies are lower. Prior to the availability of reliable electronic structure calculations, several researchers[60−62] postulated that the lower activation energies for the exo-channel are the result of a transition state structure that allows for more favorable orbital overlap at the addition site. To investigate this, the transition state structures for the endo- and exo-reactions of the simplest alkenyl radicals are shown in Figure 11; the barriers for these reactions are provided in parentheses. The reaction coordinate involves three participating atoms: the radical site in the reactant ("x"), the addition site ("1" for endo and "2" for exo), and the radical site in the product ("2" for endo and "1" for exo). In the endo-structures,

DOI: 10.1021/jp511017z
J. Phys. Chem. A XXXX, XXX, XXX−XXX

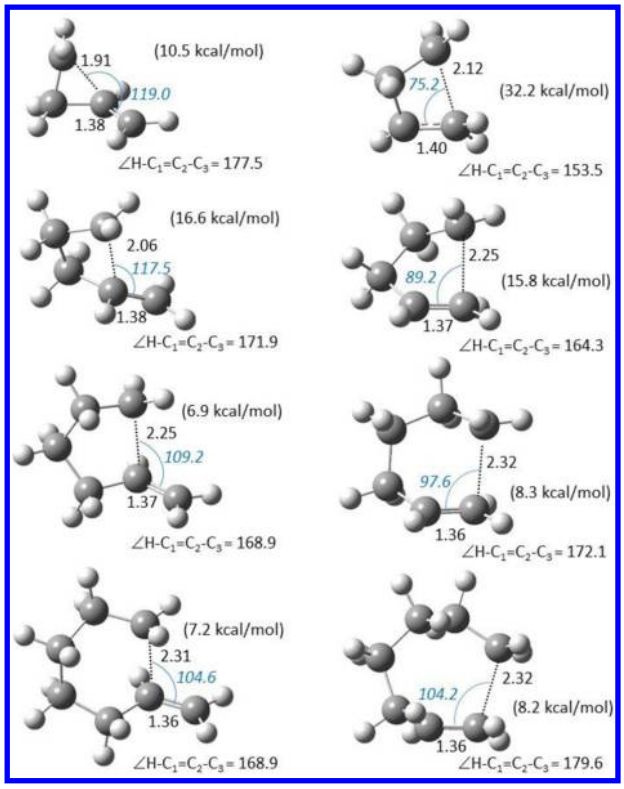

Figure 11. Transition state structures for the exo- (left) and endo- (right) cycloaddition reactions of the simplest alkenyl radicals.

all three of the participating atoms are contained within the ring; in the exo-structures only two of the reacting atoms are in the ring, while the third is outside of the ring. Bond formation occurs by overlap of the singly occupied molecular orbital (SOMO) on the radical site with the π^* orbital of the olefin. Comparison of the two sets of transition states does indeed show that the orbital overlap is more favorable in the exo-structures, especially in the 1,4- and 1,5-reactions. In these cases, the endo-transition states appear to be disfavored because in order to obtain sufficient orbital overlap, the double bond must rotate out of the plane more so than it does in the exo-structures. For instance, in the 1,4-exo-transition state structure, the angle between the radical site and the 1-carbon is obtuse, and the H−C_1═C_2−C_3 dihedral is just slightly out of the plane at 177.5°. In contrast, in the competing endo-structure, the angle between the radical site and the 2-carbon is acute. The carbon chain must reach over the double bond resulting in an H−C_1═C_2−C_3 dihedral angle of 153.5°. As a result, the newly formed bond is much longer in the endo-structure (C_1−C_4 = 2.12 Å) than it is in the exo-structure (C_2−C_4 = 1.91 Å). The same trends are observed for the 1,5-cycloadditions. As the ring size is increased in the 1,6- and 1,7-reactions, the barriers for the two channels become comparable.

Based on the above explanation, one might expect that the ring strains for the exo-transition states would be more "typical" and that those for the endo-transition states would be higher than "typical". However, the results presented here show that ring strains for the exo-transition state ring strains are unusually low (see Table 9). This is especially the case for the formation of three- and four-member ring structures, with the three-member ring having less strain than the four-member ring. In contrast, the ring strain energies for the endo-reactions are similar to those for the H atom shift reactions. Thus, there appears to be some favorable interaction in the exo-transition states that either reduces or offsets the ring strain energy in a way that cannot be explained by the above rationale. Recently, Wang et al.[35] examined the Hirshfeld atomic charge distribution for the reactants, products, and transition states for the 1,4-, 1,5-, and 1,6-exo-cycloaddition reactions. They suggest that the low barrier for the formation of the three-membered ring is attributed to a decrease in the stability in the alkene-4-yl reactant due to a stronger inductive effect of the double bond, as well as an increase in the stability in the transition state due to extra conjugative effects.

Even though the exo-cycloaddition reactions are generally favored over the endo-pathways, an important question to ask is what roles do the two pathways play during reactions of hydrocarbons? To evaluate this, one has to consider the subsequent reactions of the cycloalkyl radical products as well as other the competing reaction channels of the alkenyl radical. To illustrate this, consider the reactions of 1-pent-4-enyl radical (C═CCCC•), which can be formed from allyl addition to ethylene. A simplified version of the C_5H_9 PES is provided in Figure 12. The barriers for both cycloaddition reactions are

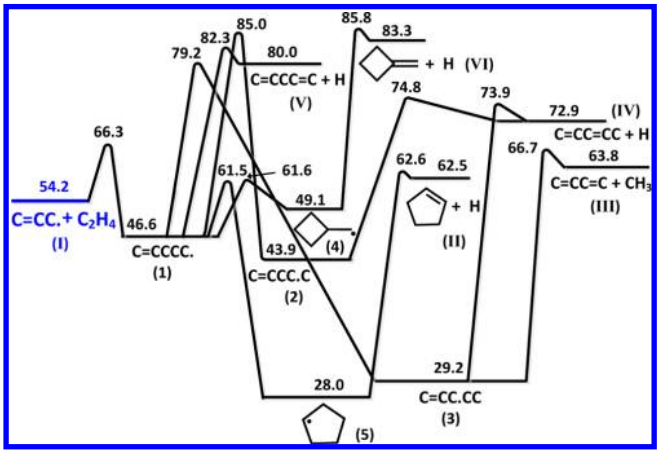

Figure 12. Potential energy surface for C_5H_9 calculated at the CBS-QB3 level of theory, showing the enthalpies in kcal/mol at 298 K.

lower than the competing H atom shifts (including from the allylic site) and β-scission reactions. While the two cycloaddition barriers are comparable, the pre-exponential factor for the formation of the cyclobutyl-carbinyl radical (4) via the exo-pathway is over an order of magnitude larger than the formation of cyclopentyl radical (5) via the endo-pathway. However, once formed, the cyclobutyl-carbinyl radical (4) is more likely to ring-open back to the 1-pent-4-eneyl radical (1) than it is to β-scission to form methylene-cyclobutane plus H (VI). In contrast, the β-scission barrier for cyclopentyl radical (5) to form cyclopentene plus H (II) is comparable to that for ring opening to (1). Thus, in this case, the endo-cycloaddition appears to be more important in the degradation of alkenyl radicals than the exo-cycloaddition channel. A more detailed discussion of this PES, which includes an analysis of the pressure-dependence of the various reaction channels, has recently been provided.[28] A comparison between predicted and experimental[63] measurements for the rate constant for formation of cyclopentene + H (II) from the reaction of allyl + C_2H_4 (I) is shown in the Supporting Information, Figure S8.

The overall importance of the various channels (cycloadditions, H-shifts, and β-scissions) depends upon the distance

DOI: 10.1021/jp511017z
J. Phys. Chem. A XXXX, XXX, XXX−XXX

between the radical site and double bond in the alkenyl radical as well as its structure. Depending on the structure of the alkenyl radical, the ring opening reactions can shift the position of the vinyl group; these types of isomerizations have been discussed by Wang et al.[35] Another important factor is the need to consider competing bimolecular reactions. Thus, it is important to include all of these reactions in kinetic modeling studies. The pressure dependence of these reactions should also be considered.

CONCLUSIONS

A systematic series of high-pressure rate rules were developed for the H atom shift reactions of alkyl radicals and the cycloaddition reactions of alkenyl radicals. These rules are based on the results of CBS-QB3 calculations and transition state theory calculations. The calculated values fall into well-defined groups that permit the assignment of a single rate constant for the group. The results are in good agreement with available literature data. The trends in the activation energies and pre-exponential factors were discussed in the context of the Benson-type model. The ring strain energies for the exo-cycloaddition reactions were found to be unusually low. The ring strain energies for the endo-cycloaddition and H-shift reactions are comparable to one another and to the ring strain of the corresponding cycloalkanes for three- to six-member rings. However, the larger sized ring strains are lower than those of the corresponding cycloalkanes. The pre-exponential factors for both the H-shift and cycloaddition reactions decrease by almost an order of magnitude with each additional hindered rotor that is frozen in the transition state structure. The structure−reactivity relationships that are developed here provide a straightforward means to assign rate constants in mechanisms as well as to be able to quickly assess the validity of proposed rate constants.

ASSOCIATED CONTENT

Supporting Information

Plots of the calculated rate constants for the various 1,*x*-H shift reactions of *n*-alkyl radicals (Figure S1) and the various 1,*x*-endo- and exo-cycloaddition reactions (Figures S3 and S4, respectively) are provided. Comparisons between the rate constants calculated in this work to experiment and calculated data in the literature for H-shift reactions (Figure S2), ring opening reactions (Figure S5), exo-cycloaddition reactions (Figure S6), and H-abstraction reactions (Figure S7) are also provided. A comparison between prediction and experiment measurement for the formation of cyclopentene + H from the reaction of allyl + C_2H_4 is shown in Figure S8. This material is available free of charge via the Internet at http://pubs.acs.org.

AUTHOR INFORMATION

Corresponding Author

*E-mail: amdean@mines.edu; Tel.: (303) 273-3643.

Notes

The authors declare no competing financial interest.

ACKNOWLEDGMENTS

The authors wish to thank Prof. Hans-Heinrich Carstensen at Ghent University for assistance with the rate constant calculations and Prof. G. Barney Ellison at the University of Colorado Boulder for helpful discussions. This work was supported by the Petroleum Institute and the National Advanced Biofuels Consortium.

REFERENCES

(1) Benson, S. W. *Thermochemical Kinetics*, 2nd ed.; Wiley: New York, 1976.
(2) Tsang, W.; McGivern, W. S.; Manion, J. A. Multichannel Decomposition and Isomerization of Octyl Radicals. *Proc. Combust. Inst.* **2009**, *32*, 131−138.
(3) Hayes, C. J.; Burgess, D. R., Jr. Kinetic Barriers of H-atom Transfer Reactions in Alkyl, Allylic, and Oxoallylic Radicals as Calculated by Composite Ab Initio Methods. *J. Phys. Chem. A* **2009**, *113*, 2473−2482.
(4) Davis, A. C.; Francisco, J. S. Ab Initio Study of Hydrogen Migration across n-Alkyl Radicals. *J. Phys. Chem. A* **2011**, *115*, 2966−2977.
(5) Sirjean, B.; Dames, E.; Wang, H.; Tsang, W. Tunneling in Hydrogen-Transfer Isomerization of n-Alkyl Radicals. *J. Phys. Chem. A* **2012**, *116*, 319−332.
(6) Endrenyi, L.; Le Roy, D. J. The Isomerization of n-Pentyl and 4-Oxo-1-Pentyl Radicals in the Gas Phase. *J. Phys. Chem.* **1966**, *70*, 4081−4084.
(7) Watkins, K. W. Photolysis of n-Pentylazomethane Vapor. Reactions of the n-Pentyl Radical. *J. Am. Chem. Soc.* **1971**, *93*, 6355−6359.
(8) Watkins, K. W. On the Rate Constant for n-Pentyl Radical Isomerization. *Can. J. Chem.* **1972**, *50*, 3738−3740.
(9) Marshall, R. M. The Rate Constant for the Intramolecular Isomerization of Pentyl Radicals. *Int. J. Chem. Kinet.* **1990**, *22*, 935−950.
(10) Yamauchi, N.; Miyoshi, A.; Kosaka, K.; Koshi, M.; Matsui, N. Thermal Decomposition and Isomerization Processes of Alkyl Radicals. *J. Phys. Chem. A* **1999**, *103*, 2723−2733.
(11) Miyoshi, A.; Widjaja, J.; Yamauchi, N.; Koshi, M.; Matsui, H. Direct Investigations on the Thermal Unimolecular Isomerization Reaction of 1-Pentyl Radicals. *Proc. Combust. Inst.* **2002**, *29*, 1285−1293.
(12) Watkins, K. W.; Ostreko, L. A. Isomerization of n-Hexyl Radicals in the Gas Phase. *J. Phys. Chem.* **1969**, *73*, 2080−2083.
(13) Dobe, S.; Berces, T.; Reti, F.; Marta, F. Isomerization of n-Hexyl and s-Octyl Radicals by 1,5 and 1,4 Intramolecular Hydrogen Atom Transfer Reactions. *Int. J. Chem. Kinet.* **1987**, *19*, 895−921.
(14) Imbert, F. E.; Marshall, R. M. The Mechanism and Rate Parameters for the Pyrolysis of n-Hexane in the Range 723−823 K. *Int. J. Chem. Kinet.* **1987**, *19*, 81−103.
(15) Tsang, W.; Walker, J. A.; Manion, J. A. Single-Pulse Shock-Tube Study on the Decomposition of 1-Pentyl Radicals. *Symp. (Int.) Combust.* **1998**, *1*, 135−142.
(16) Miyoshi, A.; Yamauchi, N.; Kosaka, K.; Koshi, M.; Matsui, H. Two-Channel Thermal Unimolecular Decomposition of Alkyl Iodides. *J. Phys. Chem. A* **1999**, *103*, 46−53.
(17) Tsang, W.; Walker, J. A.; Manion, J. A. The Decomposition of Normal Hexyl Radicals. *Proc. Comb. Inst.* **2007**, *31*, 141−148.
(18) McGivern, W. S.; Awan, I. A.; Tsang, W.; Manion, J. A. Isomerization and Decomposition Reactions in the Pyrolysis of Branched Hydrocarbons: 4-Methyl-1-Pentyl Radical. *J. Phys. Chem. A* **2008**, *112*, 6908−6917.
(19) Tsang, W.; Awan, I.; McGovern, S.; Manion, J. A. Soot Precursors from Real Fuels: The Unimolecular Reactions of Fuel Radicals. In *Combustion Generated Fine Carbon Particles*; Bockhorn, H., D'Anna, A., Sarofim, A. F., Wang, H., Eds.; KIT Scientific Publishing: Karlsruhe, Germany, 2009; pp 55−74.
(20) Wang, F.; Cao, D. B.; Liu, G.; Ren, J.; Li, Y. W. Theoretical Study of the Competitive Decomposition and Isomerization of 1-Hexyl Radical. *Theor. Chem. Acc.* **2010**, *126*, 87−98.
(21) Chen, L.; Wang, W. N.; Li, C. Y.; Lü, J.; Wang, W. L. Thermal Decomposition and Isomerization of 1-Heptyl Radical: A Computational Investigation. *Theor. Chem. Acc.* **2014**, *133*, 1509.

DOI: 10.1021/jp511017z
J. Phys. Chem. A XXXX, XXX, XXX−XXX

(22) Awan, I. A.; Burgess, D. R., Jr.; Manion, J. A. Pressure Dependence and Branching Ratios in the Decomposition of 1-Pentyl Radicals: Shock Tube Experiments and Master Equation Modeling. *J. Phys. Chem. A* **2012**, *116*, 2895−2910.
(23) Bankiewicz, B.; Huynh, L. K.; Ratkiewicz, A.; Truong, T. N. Kinetics of 1,4-Hydrogen Migration in the Alkyl Radical Reaction Class. *J. Phys. Chem. A* **2009**, *113*, 1564−1573.
(24) Ratkiewicz, A.; Bankiewicz, B. Kinetics of 1,5-Hydrogen Migration in Alkyl Radical Reaction Class. *J. Phys. Chem. A* **2012**, *116*, 242−254.
(25) Ratkiewicz, A.; Bankiewicz, B.; Truong, T. N. Kinetics of Thermoneutral Intermolecular Hydrogen Migration in Alkyl Radicals. *Phys. Chem. Chem. Phys.* **2010**, *12*, 10988−10995.
(26) Matheu, D. M.; Green, W. H.; Grenda, J. M. Capturing Pressure-Dependence in Automated Mechanism Generation: Reactions Through Cycloalkyl Intermediates. *Int. J. Chem. Kinet.* **2003**, *35*, 95−119.
(27) Davis, A. C.; Francisco, J. S. Ab Initio Study of Key Branching Reactions in Biodiesel and Fischer−Tropsch Fuels. *J. Am. Chem. Soc.* **2011**, *133*, 19110−19124.
(28) Wang, K.; Villano, M. S.; Dean, M. A. Reactions of Allylic Radicals that Impact Molecular Weight Growth Kinetics. *Phys. Chem. Chem. Phys.* **2015**, in press.
(29) Arnold, P. A.; Carpenter, B. K. Computational Studies on the Ring Openings of Cyclopropyl Radical and Cyclopropyl Cation. *Chem. Phys. Lett.* **2000**, *328*, 90−96.
(30) Olivella, S.; Sole, A.; Bofill, J. M. A Theoretical Investigation of the Thermal Ring Opening of Cyclopropyl Radical into Allyl Radical. Evidence for a Highly Nonsymmetric Transition State. *J. Am. Chem. Soc.* **1990**, *112*, 2160−2167.
(31) Smith, D. M.; Nicolaides, A.; Golding, B. T.; Radom, L. Ring Opening of the Cyclopropylcarbinyl Radical and its N- and O-Substituted Analogues: A Theoretical Examination of Very Fast Unimolecular Reactions. *J. Am. Chem. Soc.* **1998**, *120*, 10223−10233.
(32) Cooksy, A. L.; King, H. F.; Richardson, W. H. Molecular Orbital Calculations of Ring Opening of the Isoelectronic Cyclopropylcarbinyl Radical, Cyclopropoxy Radical, and Cyclopropylaminium Radical Cation Series of Radical Clocks. *J. Org. Chem.* **2003**, *68*, 9441−9452.
(33) Sirjean, B.; Glaude, P. A.; Ruiz-Lopèz, M. F.; Fournet, R. Theoretical Kinetic Study of Thermal Unimolecular Decomposition of Cyclic Alkyl Radicals. *J. Phys. Chem. A* **2008**, *112*, 11598−11610.
(34) Baldwin, J. E. Rules for Ring Closure. *J. Chem. Soc., Chem. Commun.* **1976**, 734−736.
(35) Wang, Z. H.; Zhang, L. D.; Zhang, F. Kinetics of Homoallylic/Homobenzylic Rearrangement Reactions under Combustion Conditions. *J. Phys. Chem. A* **2014**, *118*, 6741−6748.
(36) Frisch, M. J.; Trucks, G. W.; Schlegel, H. B.; Scuseria, G. E.; Robb, M. A.; Cheeseman, J. R.; Montgomery, J. A., Jr.; Vreven, T.; Kudin, K. N.; Burant, J. C., et al. *Gaussian 03*, Revision A.1; Gaussian, Inc: Pittsburgh, PA, 2003.
(37) Frisch, M. J.; Trucks, G. W.; Schlegel, H. B.; Scuseria, G. E.; Robb, M. A.; Cheeseman, J. R.; Scalmani, G.; Barone, V.; Mennucci, B.; Petersson, G. A., et al. *Gaussian 09*, Revision A.1, Gaussian, Inc: Wallingford, CT, 2009.
(38) Montgomery, J. J. A.; Frisch, M. J.; Ochterski, J. W.; Petersson, G. A. A Complete Basis Set Model Chemistry. VII. Use of the Minimum Population Localization Method. *J. Chem. Phys.* **2000**, *112*, 6532−6542.
(39) East, A. L. L.; Radom, L. Ab Initio Statistical Thermodynamical Models for the Computation of Third-Law Entropies. *J. Chem. Phys.* **1997**, *106*, 6655−6674.
(40) Villano, S. M.; Huynh, L. K.; Carstensen, H.-H.; Dean, A. M. High-Pressure Rate Rules for Alkyl + O_2 Reactions. 1. The Dissociation, Concerted Elimination, and Isomerization Channels of the Alkyl Peroxy Radical. *J. Phys. Chem. A* **2011**, *115*, 13425−13442.
(41) Villano, S. M.; Huynh, L. K.; Carstensen, H.-H.; Dean, A. M. High-Pressure Rate Rules for Alkyl + O_2 Reactions. 2. The Isomerization, Cyclic Ether Formation, and β-Scission Reactions of Hydroperoxy Alkyl Radicals. *J. Phys. Chem. A* **2012**, *116*, 5068−5089.
(42) Carstensen, H.-H.; Dean, A. M. Rate Constant Rules for the Automated Generation of Gas-Phase Reaction Mechanisms. *J. Phys. Chem. A* **2009**, *113*, 367−380.
(43) Eckart, C. The Penetration of a Potential Barrier by Electrons. *Phys. Rev.* **1930**, *35*, 1303−1309.
(44) Pollak, E.; Pechukas, P. Symmetry Numbers, Not Statistical Factors, Should Be Used in Absolute Rate Theory and in Broensted Relations. *J. Am. Chem. Soc.* **1978**, *100*, 2984−2991.
(45) Coulson, D. R. Statistical Factors in Reaction Rate Theories. *J. Am. Chem. Soc.* **1978**, *100*, 2992−2996.
(46) Pfaendter, P.; Yu, X.; Broadbelt, L. J. The 1-D Hindered Rotor Approximation. *Theor. Chem. Acc.* **2007**, *118*, 881−898.
(47) Carpenter, B. K. Ab Initio Computation of Combustion Kinetics. 1. Vinyl Radical + O_2. *J. Phys. Chem.* **1995**, *99*, 9801−9810.
(48) Chan, W.-T.; Pritchard, H. O.; Hamilton, I. P. Dissociative Ring-Closure in Aliphatic Hydroperoxyl Radicals. *Phys. Chem. Chem. Phys.* **1999**, *1*, 3715−3719.
(49) Dolbier, W. R., Jr. Structure, Reactivity, and Chemistry of Fluoroalkyl Radicals. *Chem. Rev.* **1996**, *96*, 1557−1584 and references therein..
(50) Dolbier, W. R., Jr.; Rong, X. X.; Bartgerger, M. D.; Koroniak, H.; Smart, B. E.; Yang, Z. Y. Cyclization Reactivities of Fluorinated Hex-5-Enyl Radicals. *J. Chem. Soc. Perkin Trans. 2* **1998**, *2*, 219−232.
(51) Dolbier, W. R., Jr.; Rong, X. X.; Smart, B. E.; Yang, Z. Y. Rate of Cyclization of Perfluoro-4-Oxa-5-hexenyl Radical. Use of Tributylgermanium Hydride as an Effective H-Transfer Agent for Perfluoro-n-Alkenyl Radicals. *J. Org. Chem.* **1996**, *61*, 4824−4826.
(52) Dolbier, W. R., Jr.; Li, A.; Smart, B. E.; Yang, Z. Y. Remarkable Cyclization Reactivities of Partially-Fluorinated 6-Heptenyl Radicals. *J. Org. Chem.* **1998**, *63*, 5687−5688.
(53) Li, A.; Shatrev, A. B.; Smart, B. E.; Yang, Z. Y.; Lusztyk, J.; Ingold, K. U.; Bravo, A.; Dolbier, W. R., Jr. Cyclizations of 5-Hexenyl, 6-Heptenyl, 7-Octenyl, and 8-Nonenyl Radicals. The Kinetic and Regiochemical Impact of Fluorine and Oxygen Substituents. *J. Org. Chem.* **1999**, *64*, 5993−5999.
(54) Gierczak, T.; Gawłowski, J.; Niedzielski, J. Mutual Isomerization of Cyclopentyl and 1-Penten-5-y1 Radicals. *Int. J. Chem. Kin.* **1986**, *18*, 623−637.
(55) Tsang, W. Mechanism and Rate Constants for the Decomposition of 1-Pentenyl Radicals. *J. Phys. Chem. A* **2006**, *110*, 8501−8509.
(56) Handford-Styring, S. M.; Walker, R. W. Addition of Cyclopentane to Slowly Reacting Mixtures of H_2 + O_2 Between 673 and 783 K: Reactions of H and OH with Cyclopentane and of Cyclopentyl Radicals. *J. Chem. Soc. Faraday Trans.* **1995**, *91*, 1431−1438.
(57) Chatgilialoglu, C.; Ingold, K. U.; Scaiano, J. C. Rate Constants and Arrhenius Parameters for the Reactions of Primary, Secondary, and Tertiary Alkyl Radicals with Tri-n-Butyltin Hydride. *J. Am. Chem. Soc.* **1981**, *103*, 7739−7742.
(58) Wu, C.-W.; Chen, H.-L; Ho, J.-J. The Calculated Effects of Substitution on Intramolecular Cyclization of 2,5-Hexadienyl Radicals. *J. Mol. Struct.: THEOCHEM* **2007**, *815*, 11−20.
(59) Cohen, N. J. Revised Group Additivity Values for Enthalpies of Formation (at 298 K) of Carbon-Hydrogen and Carbon-Hydrogen-Oxygen Compounds. *Phys. Chem. Ref. Data* **1996**, *25*, 1411−1481.
(60) Beckwith, A. L. J.; Schiesser, C. H. Regio- and Stereo-Selectivity of Alkenyl Radical Ring Closure: A Theoretical Study. *Tetrahedron* **1985**, *41*, 3925−3941.
(61) Beckwith, A. L. J. Regio-Selectivity and Stereo-Selectivity in Radical Reactions. *Tetrahedron* **1981**, *31*, 3073−3100.
(62) Beckwith, A. L. J.; Schiesser, C. H. A Force-Field Study of Alkenyl Radical Ring Closure. *Tetrahedron Lett.* **1985**, *26*, 373−376.
(63) Sakai, T.; Nohara, D.; Kunugi, T. In *Industrial and Laboratory Pyrolysis*; American Chemical Society: Washington, DC, 1976; Chapter 10, pp 152−177.

DOI: 10.1021/jp511017z
J. Phys. Chem. A XXXX, XXX, XXX−XXX